Sonic hedgehog regulates its own receptor on postcrossing commissural axons in a glypican1-dependent manner

Wilson, Nicole H ; Stoeckli, Esther T

Abstract: Upon reaching their intermediate target, the floorplate, commissural axons acquire responsiveness to repulsive guidance cues, allowing the axons to exit the midline and adopt a contralateral, longitudinal trajectory. The molecular mechanisms that regulate this switch from attraction to repulsion remain poorly defined. Here, we show that the heparan sulfate proteoglycan Glypican1 (GPC1) is required as a coreceptor for the Shh-dependent induction of Hedgehog-interacting protein (Hhip) in commissural neurons. In turn, Hhip is required for postcrossing axons to respond to a repulsive anteroposterior Shh gradient. Thus, Shh is a cue with dual function. In precrossing axons it acts as an attractive guidance molecule in a transcription-independent manner. At the same time, Shh binds to GPC1 to induce the expression of its own receptor, Hhip, which mediates the repulsive response of postcrossing axons to Shh. Our study characterizes a molecular mechanism by which navigating axons switch their responsiveness at intermediate targets.

DOI: https://doi.org/10.1016/j.neuron.2013.05.025

Sonic hedgehog regulates its own receptor on post-crossing commissural axons in a Glypican1-dependent manner

Nicole H. Wilson[1] and Esther T. Stoeckli[1]

[1]University of Zurich

Institute of Molecular Life Sciences

Winterthurerstrasse 190

CH-8057 Zurich, Switzerland

Contact: Esther.Stoeckli@imls.uzh.ch

Running title:

Canonical Shh signaling regulates axon guidance

Summary

Upon reaching their intermediate target, the floorplate, commissural axons acquire responsiveness to repulsive guidance cues, allowing the axons to exit the midline and adopt a contralateral, longitudinal trajectory. The molecular mechanisms that regulate this switch from attraction to repulsion remain poorly defined. Here, we show that the heparan sulfate proteoglycan Glypican1 (GPC1) is required as a co-receptor for the Shh-dependent induction of Hedgehog-interacting protein (Hhip) in commissural neurons. In turn, Hhip is required for post-crossing axons to respond to a repulsive antero-posterior Shh gradient. Thus, Shh is a cue with dual function. In pre-crossing axons it acts as an attractive guidance molecule in a transcription-independent manner. At the same time, Shh binds to GPC1 to induce the expression of its own receptor, Hhip, which mediates the repulsive response of post-crossing axons to Shh. Our study characterizes a novel molecular mechanism by which navigating axons switch their responsiveness at intermediate targets.

Highlights

- Knockdown of GPC1 in commissural neurons perturbs axon guidance at the midline
- GPC1 genetically interacts with Shh in post-crossing commissural axon guidance
- GPC1 regulates expression of Hhip, the receptor mediating repulsion to Shh
- Switching axonal responsiveness at the midline involves Hhip induction by Shh

Introduction

During neural circuit formation, axons must navigate along stereotypical pathways in order to connect appropriately with their targets. Along these pathways they contact one or several intermediate targets at which they change their responses to guidance cues. The floorplate at the ventral midline serves as an intermediate target for dorsal commissural (dI1) neurons of the spinal cord. Commissural axons grow towards and across the floorplate, then make a sharp turn into the longitudinal axis and grow rostrally along the contralateral floorplate border (Chédotal, 2011). The initial ventral trajectory of dI1 axons is directed by a collaboration between repulsive, roofplate-derived Draxin (Islam et al., 2009) and BMPs (bone morphogenetic proteins; Augsburger et al., 1999) as well as the floorplate-derived attractants Sonic hedgehog (Shh; Charron et al., 2003) and Netrin-1 (Kennedy et al., 1994). Floorplate crossing is mediated by the short-range guidance cues Contactin2 (also known as Axonin1 or TAG-1) and NrCAM (Stoeckli and Landmesser, 1995). Upon reaching the floorplate, dI1 axons lose responsiveness to the attractive cues and gain responsiveness to repulsive cues, including Semaphorins and Slits (Zou et al., 2000; Nawabi et al., 2010). A variety of guidance cues have been implicated in post-crossing axon guidance: in addition to the cell adhesion molecules SynCAMs (Niederkofler et al., 2010) and MDGA2 (Joset et al., 2011), morphogens of the Wnt family (Lyuksyutova et al., 2003; Domanitskaya et al., 2010) and Shh (Bourikas et al., 2005; Yam et al., 2012) have been identified.

Although it is clear that axons dramatically change their guidance properties upon crossing the midline, the molecular mechanisms underlying this change in responsiveness remain poorly defined. One molecule, Shh, is not only an attractant for pre-crossing commissural

axons but is also a repulsive guidance cue for post-crossing commissural axons. Thus, at the intermediate target, the axonal response to Shh switches from attraction to repulsion.

The chemoattractive activity of Shh is mediated by Smoothened (Smo) and Boc (Charron et al., 2003; Okada et al., 2006), while the repulsive activity of Shh is mediated by Hedgehog-interacting protein (Hhip) (Bourikas et al., 2005). However, it is unknown how this receptor switch is achieved. Here, we demonstrate a role for the heparan sulfate proteoglycan (HSPG) Glypican1 (GPC1) in the transcriptional activation of the Shh receptor *Hhip*, and thus, its regulatory role in converting the Shh responsiveness of commissural axons from attraction to repulsion.

Results

GPC1 mediates commissural axon guidance

Glypicans are GPI-anchored HSPGs that have been implicated in morphogen signaling in invertebrates and vertebrates (Filmus et al., 2008). The six family members found in vertebrates have been subdivided into two classes with different, often opposite effects on morphogens. Whereas GPC3 was found to inhibit Shh signaling, the GPC1 ortholog Dally-like was found to be a positive regulator of hedgehog signaling (Beckett et al., 2008). Based on its expression in dI1 commissural neurons and in the floorplate (Figure 1A-B), GPC1 was a good candidate as a regulator of Shh activity. Of the six *GPCs* expressed in chick, only *GPC1* was found in mature commissural neurons (Figure S1).

To evaluate the role of GPC1 in the guidance of commissural axons, we performed unilateral

knockdowns by *in ovo* electroporation of plasmids expressing artificial microRNAs (miRNAs) (Figure 1C; Figure S2) (Wilson and Stoeckli, 2011). Knockdowns were performed at Hamburger and Hamilton stage 17-18 (HH17-18; Hamburger and Hamilton, 1951), just before the onset of commissural axon growth. Since a mixture of siRNAs can produce more penetrant phenotypes (Parsons et al., 2009), we first co-electroporated a mixture of three plasmids encoding effective miRNAs against GPC1 (*mi4GPC1*, *mi6GPC1* and *mi7GPC1*; Table S1; Figure S2) or, as controls, the same amount of plasmids expressing miRNA against Luciferase (*mi1Luc* or *mi2Luc*; Table S1). DiI tracing of dorsal commissural axons in the spinal cord revealed that GPC1 knockdown caused pathfinding errors of commissural axons at the midline (Figure 1D-G). Some axons failed to enter the floorplate and stopped at the floorplate entry site in the absence of GPC1, while those that did enter often stalled within the floorplate. The axons that managed to cross to the contralateral side often failed to turn into the longitudinal axis, and occasionally even turned posteriorly instead of anteriorly. Most importantly, in contrast to correctly navigating axons, the growth cones of axons which failed to turn correctly were not biased towards the rostral direction at the floorplate exit site. The phenotype observed in embryos deficient in GPC1 was highly reminiscent of the post-crossing commissural axon phenotype seen in the absence of Shh (Bourikas et al., 2005). Only 17.9% of DiI injection sites were normal in embryos lacking GPC1, compared to 64.9% in control embryos electroporated with *mi2Luc*. The abnormal phenotypes were qualitatively similar when we electroporated a single plasmid encoding *mi7GPC1*, the most effective of eight miRNAs that were tested (Figure 1H; Figure S2B).

To test the specificity of gene silencing elicited by our miRNAs, we confirmed that the

expression of non-targeted GPC family members was unchanged (Figure S2C-E) and we performed rescue experiments using a modified, full-length *GPC1* construct that was resistant to knockdown by mi7GPC1 (GPC1ΔmiR; Figure 1I; Figure S3). When *GPC1ΔmiR* was co-electroporated with *mi7GPC1* (Figure 1J), the resulting axon guidance phenotypes were indistinguishable from controls, demonstrating that expression of GPC1ΔmiR could completely rescue the effects of knocking down endogenous GPC1 with mi7GPC1 (Figure 1K-M).

Since GPCs have been shown to regulate the signaling activity of several growth factors via their heparan sulfate (HS) chains (Bonneh-Barkay et al., 1997), we investigated whether glycanation is required for the axon guidance effect of GPC1. While expression of GPC1ΔmiRΔGAG, a mutated GPC1 that cannot be glycanated (Zhang et al., 2007) (Figure S4A), significantly rescued the axon guidance defects resulting from GPC1 silencing, the rescue effect was lower than that obtained by expression of GPC1ΔmiR (Figure 1M). Thus, optimal activity of GPC1 in axon guidance requires the HS chains, but the GPC1 core protein alone also displays some activity.

GPC1 is required in dI1 neurons

Since GPC1 was expressed in the floorplate, the source of Shh, and in the Shh-responsive dI1 neurons (Figure 1A-B), we next knocked down its expression in a cell-type specific manner in order to determine its functional relevance in each cell type (Figure 2). To achieve this, we recently developed a novel *in ovo* RNAi approach (Wilson and Stoeckli, 2011). Precise spatiotemporal control of gene knockdown is achieved by the electroporation of

plasmids in which an RNA polymerase II promoter/enhancer drives the expression of a single transcript encoding both a fluorescent protein and one or two artificial miRNAs against the gene of interest (Figure S2A). The use of different promoters enables gene knockdown in a cell type-specific manner, and the transfected cells can be accurately traced by the expression of the fluorescent reporter.

Floorplate-specific knockdown was achieved by using enhancer element III of the mouse *Hoxa1* gene to drive expression of EGFP and miGPC1 or miLuc (Wilson and Stoeckli, 2011; Figure 2A-A'). In contrast to unilateral knockdown, we found that floorplate-specific knockdown of GPC1 had no significant effect on commissural axon guidance (Figure 2B-D).

To test the activity of GPC1 in commissural neurons, we used a dI1-specific enhancer of *Math1* (mouse Atonal homologue 1) to drive expression of miGPC1 or miLuc, and membrane-localized EGFP to visualize transfected axons (Wilson and Stoeckli, 2011; Figure 2E-E'). Knockdown of GPC1 specifically in dI1 neurons caused similar defects to those observed following unilateral knockdown (Figure 2F). Fewer than 36% of DiI injection sites were normal following the dI1-specific loss of GPC1, compared with 61% in the control mi1Luc-expressing group (Figure 2G,H). Thus, axonally-expressed GPC1 is required for correct guidance of commissural axons.

GPC1 and Shh interact genetically and physically

We hypothesized that axonally-expressed GPC1 might mediate the guidance response to floorplate-derived Shh. To test this idea, we used a combination of miRNAs to demonstrate a

genetic interaction between *Shh* and *GPC1*. We reasoned that if GPC1 is required for correct signaling by Shh in axon guidance, then partial knockdown of GPC1 would enhance weak phenotypes generated by partial knockdown of Shh. This approach mimics double heterozygote studies in *Drosophila*, where genetic interactions suggest that molecules function in a common signaling pathway (for example, Kidd et al., 1999; Yang et al., 2009). Similar approaches using morpholinos in *Xenopus* and zebrafish embryos have also been reported (for example, Wilson and Key, 2006; Kee et al., 2008; Rikin et al., 2010).

An effective artificial miRNA against Shh has been described (miShh; Das et al., 2006) and we have shown that, as expected, it induces both pre- and post-crossing axon guidance errors when expressed in the floorplate at HH17 or earlier (Wilson and Stoeckli, 2011). Here, we co-electroporated *Math1-EGFPF-mi7GPC1* and *Hox-EBFP2-miShh* constructs at low concentrations to reduce GPC1 in dI1 neurons, and Shh in the floorplate (Figure 3A-A'). Under these conditions the single knockdown of each gene did not significantly affect axon guidance compared to control embryos expressing only mi1Luc. However, the concomitant knockdown of axonally-expressed GPC1 and floorplate-derived Shh led to increased defects in the guidance of post-crossing axons (Figure 3B-F; Table S2). Interestingly, we did not see any increase in ipsilateral errors (Table S2), suggesting that GPC1 does not influence the attractive activity of Shh in pre-crossing axons. This finding is in line with results from a separate series of experiments where we interfered with GPC1 expression at earlier stages (HH12-14; at least 15 hours before the commissural neurons begin to project axons), and saw no additional effects on pre-crossing axons (Table S3). In particular, we did not find axons which failed to reach the floorplate, as would be expected if GPC1 and Shh would cooperate

in the attraction of pre-crossing axons. Taken together, our results suggest that GPC1 and Shh collaborate specifically during post-crossing commissural axon guidance.

To strengthen this interpretation, we also performed experiments in which we knocked down Shh together with Contactin2 (Cntn2), a gene that acts in a different pathway to regulate midline crossing. We have previously shown that axonally-expressed Cntn2 interacts with midline-derived NrCAM to make axons enter the floorplate (Stoeckli and Landmesser, 1995; Wilson and Stoeckli, 2011). In post-crossing axons, Cntn2 interacts with NgCAM to regulate axon fasciculation (Stoeckli and Landmesser, 1995). In our combinatorial knockdown experiments, the simultaneous knockdown of genes involved in parallel pathways should not cause a significant aggravation of the single gene manipulations. In line with this reasoning, we saw no exacerbation of either pre-crossing or post-crossing axon guidance phenotypes after combinatorial knockdown of Shh and Cntn2 (Figure 3F; Table S2). These findings strongly support our conclusion that GPC1 and Shh act in the same molecular pathway to regulate post-crossing commissural axon guidance.

Next, we confirmed that GPC1 can directly bind Shh by performing co-immunoprecipitations. When cell lysates prepared from HEK293T cells co-transfected with FLAG-tagged *Shh* and HA-tagged *GPC1* constructs were incubated with anti-FLAG M2 affinity gel, GPC1 was co-precipitated (Figure 3G). These results indicated that GPC1 is capable of binding Shh.

GPC1 regulates dorsal Hhip expression

Based on previous studies in flies and vertebrates, GPC1 and Shh could cooperate in two different (but not necessarily exclusive) manners to mediate post-crossing commissural axon guidance: (i) GPC1 could directly promote or inhibit Shh's interaction with its axon guidance receptors (Beckett et al., 2008; Capurro et al., 2008; Williams et al., 2010); and/or (ii) the presence of GPC1 within a receptor complex could regulate Gli-dependent transcription and subsequent gene expression in response to Shh (Chan et al., 2009), which in turn would specify the expression of guidance receptors on commissural axons. Here, we investigated the latter.

Gene transcription has been demonstrated to regulate discrete steps in post-commissural axon guidance (Condron, 2002), and Shh has been speculated to be an appropriate floorplate-derived signal that could induce such an activity (Sanchez-Camacho and Bovolenta, 2009). However, so far evidence for such a mechanism has been elusive. Our previous studies identified Hhip as a mediator of the repulsive guidance response to Shh (Bourikas et al., 2005). *Hhip* mRNA is detectable transiently in dI1 neurons at the time when post-crossing axons turn into the longitudinal axis (Figure S5; Bourikas et al., 2005). Interestingly, *Hhip* is a transcriptional target of Shh (Chuang and McMahon, 1999; Buttitta et al., 2003), suggesting that commissural neurons might begin to upregulate *Hhip* as they encounter high levels of Shh in the floorplate. Thus, we hypothesized that transcriptional activity in response to Shh, in a GPC1-dependent manner, could modulate the responsiveness of the commissural growth cone at this intermediate target.

To investigate this idea, we analyzed *Hhip* mRNA expression patterns in the spinal cord

following GPC1 knockdown. Strikingly, we found that embryos electroporated with *βact-hrGFPII-mi7GPC1* (Figure 4A) or *βact-hrGFPII-mi4GPC1* (data not shown) displayed a specific loss of *Hhip* expression in the dorsal spinal cord on the electroporated side. In contrast, ventromedial *Hhip* expression was unaffected by the loss of GPC1, demonstrating a cell-type specific requirement for GPC1 in *Hhip* induction. Electroporation of a control plasmid, *βact-hrGFPII-mi2Luc*, did not affect *Hhip* expression (Figure 4B). Rescue experiments, as described above, revealed that dorsal expression of *Hhip* could be restored by the expression of GPC1ΔmiR (Figure 4C-F).

We quantified these effects using two methods. First, we calculated the percentage of sections in each condition displaying 'symmetrical' versus 'asymmetrical' *Hhip* levels in the dorsal spinal cord (Figure 4C-F, % values indicate the number of sections with symmetrical expression). Alternatively, we digitally analyzed pixel intensity in the dorsal and medial spinal cord and calculated the ratios of pixels on the electroporated side versus the untreated side (PI^{elect}:$PI^{control}$) for the dorsal and medial areas (Figure 4G). Both methods indicated that *Hhip* expression was significantly reduced in the dorsal spinal cord following knockdown of GPC1, and that this effect could be rescued by expressing GPC1ΔmiR. GPC1ΔmiRΔGAG elicited a partial rescue of *Hhip* expression (Figure 4F-G), consistent with its ability to partially rescue the axon guidance defects arising from GPC1 knockdown (Figure 1M).

We next determined whether the post-crossing axon guidance effects of GPC1 could be attributable to its ability to induce Hhip expression. We co-electroporated *βact-EBFP2-mi7GPC1* with *pMES-Hhip*, and found that indeed, this treatment significantly rescued the

axon guidance effects of GPC1 knockdown (Figure 4H-I; compare to Figure 1K-M). Thus, GPC1 was required to induce Hhip expression in commissural neurons, which in turn mediated the guidance response of post-crossing axons along the longitudinal axis.

To determine whether GPC1 was required cell autonomously to induce *Hhip* expression in dI1 neurons, we examined embryos electroporated with *Math1-EGFPF-mi7GPC1* (Figure 4J). In these embryos, *Hhip* was again reduced or absent in the dorsal spinal cord on the electroporated side (average PI^{elect}:$PI^{control}$ = 0.56 +/- 0.10 SEM), whereas electroporation of the control *Math1-EGFPF-mi1Luc* construct had no effect (average PI^{elect}:$PI^{control}$ = 0.99 +/- 0.09 SEM). This result was consistent with the neuron-specific requirement for GPC1 in commissural axon guidance (Figure 2).

We ruled out the possibility that the GPC1-dependent loss of *Hhip* expression was a result of gross patterning defects of the spinal cord, as the expression of markers such as Pax3 and Islet1 were unchanged (Figure S6). Similarly, we observed no difference in the expression of *Cntn2* (which is normally found in dI1 neurons) between the control and electroporated sides (Figure S6C), showing that the loss of *Hhip* expression in the dorsal spinal cord was a direct and specific consequence of GPC1 knockdown.

Shh induces Hhip via GPC1 in dI1 neurons

Taken together, these experiments demonstrated that the induction of *Hhip* expression in commissural neurons was dependent on GPC1. Next, we confirmed that *Hhip* induction occurred downstream of canonical Shh signaling. The highly dynamic expression pattern of

Hhip in the dorsal spinal cord (Figure S5) prevented accurate comparisons of *Hhip* levels between embryos; hence, we used the non-electroporated side of the spinal cord as an internal control. Because Shh is diffusible, the unilateral knockdown of Shh would not restrict its effect to the electroporated side. In other words, effective perturbation of Shh expression at the ventral midline would require bilateral electroporation of *miShh*, thus eliminating our internal control. To overcome this problem, we instead electroporated constructs encoding components of the canonical Shh pathway and assessed *Hhip* levels afterwards. When constructs encoding *Smo-M2* (a constitutively active Smo; Hynes et al., 2000), *Gli1* or *Gli2* were electroporated, *Hhip* expression was expanded ectopically (Figure 5A). Conversely, unilateral repression of canonical Shh signaling by Ptc∆loop2 (a Hedgehog-insensitive dominant repressor of Smo; Briscoe et al., 2001) caused a specific loss of dorsal *Hhip* expression (Figure 5B). This effect was identical to that observed following the loss of GPC1, but occurred with even higher penetrance and severity (compare % values in Figure 5B to Figure 4D; compare Figure 5E to Figure 4G). Thus, as predicted, *Hhip* induction in the dorsal spinal cord was dependent on Shh transcriptional activity. In line with our hypothesis, which predicted that GPC1 was acting downstream of Shh to induce *Hhip* in commissural neurons, repression of the canonical Shh pathway phenocopied the effects of GPC1 silencing.

To establish a more direct link between Shh and GPC1 in *Hhip* induction, we next tested the ability of a Shh-insensitive GPC1 mutant (GPC1ΔmiRΔGAG∆Shh) to rescue dorsal *Hhip* expression following knockdown of endogenous GPC1. The GPC1 mutant was resistant to knockdown, lacked the GAG attachment sites, and was unable to activate Shh signaling due to ablation of 10 critical amino acids (Kim et al., 2011). Unlike GPC1ΔmiR and

GPC1ΔmiRΔGAG, this construct was incapable of binding Shh in co-immunoprecipitation assays (Figure 5C). Consistent with a requirement for Shh-GPC1 interaction in the induction of dorsal *Hhip*, we found that GPC1ΔmiRΔGAGΔShh was completely unable to rescue *Hhip* expression (Figure 5D; compare Figure 5E to Figure 4G). Furthermore, GPC1ΔmiRΔGAGΔShh was incapable of rescuing the axon guidance defects induced by GPC1 knockdown (Figure 6). Taken together, these results demonstrate a functional link between the GPC1/Shh-mediated induction of *Hhip* expression and commissural axon guidance.

To test whether GPC1 was simply required as a general enhancer of Shh-mediated transcription, we assessed the expression of other known Shh target genes after GPC1 knockdown (Figure 7) (Goodrich et al., 1996; Oliver et al., 2003; Tenzen et al., 2006; Domanitskaya et al., 2010). Neither *Patched1 (Ptc1)* nor *Boc* were affected by GPC1 silencing. Furthermore, there were no effects on the Wnt antagonist (and Shh transcriptional target) *Secreted frizzled-related protein1 (Sfrp1),* or on the Wnt receptor *Frizzled3 (Fzd3)*, both of which have been implicated in post-crossing axon guidance (Lyuksyutova et al., 2003; Domanitskaya et al., 2010). Importantly, these results suggested that the longitudinal guidance defects elicited by the loss of GPC1 were not due to perturbation of the chemoattractive Wnt-Fzd3 pathway (at least, not at the transcriptional level). The lack of dependence on GPC1 for transcription of *Boc*, *Ptc1* and *Sfrp1* suggested that GPC1 is required specifically for the regulation of *Hhip* expression in dI1 neurons, rather than as a general component of Shh-mediated transcriptional activation. This conclusion is supported

by our observation that *Hhip* expression was only lost in the dorsal subpopulation of cells following GPC1 knockdown (Figure 4A, G).

Finally, to demonstrate that GPC1 can influence the canonical Shh pathway during neural tube development, we examined the expression of several Shh target genes following GPC1 overexpression. *Ptc1*, *Sfrp1* and *Hhip* were all expressed ectopically after electroporation of *pMES-GPC1* (Figure 7C, D), an effect that was never observed following electroporation of a control (*pMES-empty*) plasmid. Thus, GPC1 is an enhancer of canonical Shh signaling *in vivo*.

Taken together, our results demonstrate that GPC1 has a specific function in regulating *Hhip* expression in commissural neurons, thereby eliciting a Shh-dependent change in axonal responsiveness to Shh at the midline choice point.

Discussion

In addition to identifying GPC1 as a novel regulator of commissural axon guidance, our study establishes the existence of another important Shh signaling pathway in commissural neurons: the GPC1-dependent activation of transcription, which in turn modifies the growth cone's sensitivity to floorplate-derived cues. Our findings not only highlight the remarkable multifunctionality of Shh during neural development, but also delineate a molecular mechanism by which navigating axons can switch their responses to intermediate targets.

Shh plays multiple roles in commissural axon guidance

Together with previous reports, our results provide a complex and highly dynamic picture of Shh signaling in commissural axon guidance (Figure 8). First, Shh collaborates with Netrin-1 to attract axons towards the floorplate, in a Boc-dependent manner (Charron et al., 2003; Okada et al., 2006). However, Shh not only signals via a rapid, non-canonical pathway to elicit growth cone attraction (Yam et al., 2009), but simultaneously activates a slower transcriptional pathway which triggers the upregulation of Shh-induced genes in the neurons, including (but perhaps not limited to) *Hhip*. Additionally, Shh modulates cAMP levels in commissural growth cones to confer sensitivity to repulsive Semaphorins at the midline (Parra and Zou, 2010). Shh then acts directly as a repulsive guidance cue to guide post-crossing axons anteriorly, in a Hhip-dependent manner (Bourikas et al., 2005). Finally, Shh also shapes a chemoattractive Wnt activity gradient, by inducing the graded expression of the Wnt antagonist Sfrp1 along the antero-posterior axis of the spinal cord (Domanitskaya et al., 2010).

Canonical Shh signaling is required for commissural axon guidance

Our study shows that Shh not only guides pre-crossing axons directly by binding to its receptors on the growth cone (Okada et al., 2006; Yam et al., 2009), but simultaneously activates the transcription of its own receptor, which is required for a subsequent stage of axon guidance. How could the canonical and non-canonical Shh pathways operate in parallel in pre-crossing neurons? One intriguing possibility is that Smo (which functions in both pathways), is responsible for eliciting the distinct outputs. A recent study suggests that the intracellular trafficking of Smo to distinct subcellular compartments is responsible for generating either a chemotactic or transcriptional response (Bijlsma et al., 2012). Smo on the

primary cilium appears to relay the Shh signal to Gli proteins, resulting in transcriptional activation. In contrast, Smo located outside the primary cilium controls chemotactic responses to Shh. Based on the lack of mRNA expression in mature commissural neurons at the appropriate stage of development (after HH23), we previously concluded that Ptc and Smo were not directly required to mediate the repulsive axon guidance response to Shh in post-crossing axons (Bourikas et al., 2005). Our current results reveal that these genes are in fact required indirectly for this response, since their earlier activity in commissural axons at the midline is necessary to activate transcription of *Hhip*.

Our results are consistent with a recent study indicating that interactions between Shh and proteoglycans are necessary to regulate distinct aspects of Gli-dependent transcription and gene expression (Chan et al., 2009). Of note is that GPC1 was not required in all cell types as a general enhancer of Shh transcription, since the loss of GPC1 did not affect *Boc*, *Ptc1* or *Sfrp1* levels, or even *Hhip* expression in the medial domains (Figure 4; Figure 7). Rather, dI1 neurons specifically required GPC1 to mediate a transcriptional response to Shh.

Molecular mechanisms to modulate the change in Shh responsiveness

In chick, the post-crossing repulsive axon guidance response to Shh relies on the expression of Hhip, and our study has identified the molecular pathway that regulates *Hhip* expression in commissural neurons. How is the attractive, Boc-mediated effect of Shh deactivated in post-crossing axons? There are several possibilities. The transient *Boc* expression in commissural neuron precursors may not result in persistent Boc protein levels on axons at the intermediate target (Okada et al., 2006), or Hhip expression may interfere with the attractive response

mediated by Boc. Consistent with the latter idea, alkaline phosphatase-tagged Shh binds with higher affinity to Hhip compared to Boc (Chuang and McMahon, 1999; Okada et al., 2006). Hence, the upregulation of Hhip in axons at the midline could sequester Shh away from Boc, thus favoring the activation of a repulsive Hhip-containing receptor complex. Furthermore, we do not exclude the possibility that GPC1 itself could directly promote post-crossing axon guidance by enhancing the affinity of Shh for Hhip, or promoting the formation of a Hhip-containing receptor complex (Figure 8). These possibilities remain to be tested. GPC1 does not appear to alter the expression levels of *Boc* (Figure 7A), consistent with the specific effect of GPC1 in mediating post-crossing responses to Shh (Tables S2 and S3).

During the revision of this manuscript, a report by Yam and colleagues (2012) suggested that in rodents, there is a cell-intrinsic switch in the intracellular state of the commissural growth cone, mediated by 14-3-3 adaptor proteins. In that model, 14-3-3 levels change the polarity of the turning response to Shh from attraction to repulsion, in a time-dependent manner which does not rely on extrinsic cues. Yam and colleagues (2012) also suggest that Hhip is not required for post-crossing commissural axon guidance in mice, since Hhip knockout mice did not display overt pathfinding errors. Whether 14-3-3 acts in addition to Hhip to fine-tune axon guidance responses to Shh in chick remains to be investigated. Regardless of the mechanisms, post-crossing commissural axons are clearly no longer attracted by Shh in both chick and mammals (Lyuksyutova et al., 2003; Bourikas et al., 2005; Yam et al., 2012).

The GPC1-dependent transcriptional switch in response to Shh is autoregulatory

Our study suggests that the axon guidance cue Shh regulates the expression of its own guidance receptor for the next stage of the axonal trajectory. In *Drosophila*, a switch from attraction to repulsion at the midline via transcriptional activation was demonstrated downstream of Frazzled/Dcc (Fra), the receptor mediating attraction of axons toward Netrin (Yang et al., 2009). In that study, the transcriptional change downstream of Fra was neither Netrin-dependent nor did it affect a receptor for Netrin. Rather, Fra was shown to regulate *commissureless* expression, which in turn regulates Robo-mediated Slit repulsion. In contrast, in our study a single ligand (Shh) orchestrates the expression of its own receptor (Hhip) to enable the next stage of axon pathfinding.

Shh may also affect the expression of other axon guidance receptors. Interestingly, several axon guidance molecules are induced by Shh in the cerebellum, including PlexinA2, ADAMTS1 and EphB4 (Oliver et al., 2003). Shh was shown to confer sensitivity of commissural axons to Semaphorins during midline crossing, at least in part by its ability to reduce cAMP levels (Parra and Zou, 2010). However, it is unknown whether this effect is also due to an induction of the axon guidance receptors for Semaphorins.

A novel function for GPC1 in mediating commissural axon guidance

In *Drosophila* (in which there are only two GPCs: Dally and Dally-like (Dlp)), GPC has been implicated in axon guidance. At the *Drosophila* midline, Dlp acts together with Syndecan to modulate Slit-Robo signaling (Johnson et al., 2004; Smart et al., 2011), and Dlp is required for axon guidance in the fly visual system (Rawson et al., 2005). However, a specific role for GPCs in regulating vertebrate axon guidance has not previously been reported. We also add

GPC1 to the list of vertebrate GPC family members that can bind to and regulate Shh (Capurro et al., 2008; Li et al., 2011). GPC1's regulation of Shh signaling was not entirely dependent on the presence of its GAG side chains (Figure 1M, Figure 4F-G, Figure 5C), which is consistent with the abilities of the core proteins of Dlp and GPC3 to mediate specific, cell-autonomous aspects of Shh signaling (Capurro et al., 2008; Williams et al., 2010; Yan et al., 2010).

Based on the variety of axon guidance phenotypes that we observed (Figure 1E-H), GPC1 is likely to influence other axon guidance activities in addition to those described here. The floorplate stalling phenotype, for instance, is suggestive of a possible Robo/Slit modulatory effect (Long et al., 2004). Consistent with this, GPC1 binds Slit2 with high affinity (Ronca et al., 2001), and Slit2-Robo1 signaling strictly requires binding to heparan sulfate (Hu, 2001). The modulation of other axon guidance pathways by GPC1 is of interest for future studies.

Experimental Procedures

See Extended Experimental Procedures for additional details on the experiments.

Cloning of artificial miRNA plasmids, *in ovo* electroporations, open-book preparations and DiI injections

A detailed video protocol is available online: http://www.jove.com/video/4384 (Wilson and Stoeckli, 2012). In brief, miRNA plasmids were constructed as described (Figure S2A; Wilson and Stoeckli, 2011) and electroporated at HH17-18 using a BTX ECM830 square-wave electroporator (5 pulses of 25 V, 50 msec duration). Bilateral electroporation was performed using 5 pulses of 18 V, 50 msec duration, then switching the polarity of the electrodes and repeating the electroporation. The resulting axon guidance phenotypes were assessed by axonal tracing with DiI in open-book preparations at HH25-26.

Quantification of axon guidance phenotypes

The cohorts of axons in DiI injection sites were classified as showing an 'ipsilateral' phenotype, if >30% of the axons stalled at or turned longitudinally along the ipsilateral floorplate border, a 'floorplate stalling' phenotype, if >50% of axons stalled within the floorplate, or a 'post-crossing' phenotype, if >50% of axons failed to turn and/or if axons turned caudally on the contralateral side of the floorplate.

GPC1 constructs

A cDNA clone containing the full-length (1653 bp) ORF of chicken *GPC1* was amplified by PCR (Genbank accession number KF040585). Myc or HA tags were inserted between the signal sequence and the first conserved cysteine residue. *GPC1ΔmiR* was generated by silent site-directed mutagenesis of 5 nucleotides in the *mi7GPC1* target sequence (Zheng, 2004). In *GPC1ΔmiRΔGAG*, all three putative GAG attachment sites (Zhang et al., 2007) were ablated by converting three critical serine residues to tyrosines. In *GPC1ΔmiRΔGAGΔShh*, 10 additional residues (Kim et al., 2011) were mutated to alanines using the megaprimer PCR mutagenesis method (Barik, 2002).

In situ hybridization, immunolabeling and expression analysis

In situ hybridization and immunolabeling were performed as described (Mauti et al., 2006; Wilson and Stoeckli, 2011). Staining intensities in the *Hhip* images were analyzed using ImageJ software (NIH, USA). A threshold was applied, then the integrated density of pixels in the dorsal or medial spinal cord on both the control and electroporated sides were measured.

Statistical analyses

We used the VassarStats Website for Statistical Computation (Vassar College; ©Richard Lowry 1998-2013; http://vassarstats.net/). For the analysis of open-book phenotypes, the total number of DiI sites in each condition was pooled and subjected to a one-tailed Fisher Exact test and Chi-square test of association. For graphical display, the raw phenotype counts were converted to percentages. To assess the dorsal *Hhip* expression patterns, the dorsal PI^{elect}:PI^{cont} ratios were first subjected to a single sample t-test against a hypothetical mean of 1, or compared between the relevant groups using two-sample t-tests.

Acknowledgements

We thank Silvia Arber (University of Basel, Switzerland), Avihu Klar (Hebrew University, Israel), Cathy Krull (University of Michigan, USA), Andrew McMahon (Harvard University, USA) and James Briscoe (NIMR, United Kingdom) for constructs. We thank Irwin Andermatt for inputs, discussions and critical reading of the manuscript. This work was supported by a grant from the Swiss National Science Foundation (to E.S.).

References

Augsburger, A., Schuchardt, A., Hoskins, S., Dodd, J., and Butler, S. (1999). BMPs as mediators of roof plate repulsion of commissural neurons. Neuron *24*, 127–141.

Barik, S. (2002). Megaprimer PCR. Methods Mol Biol *192*, 189–196.

Beckett, K., Franch-Marro, X., and Vincent, J.-P. (2008). Glypican-mediated endocytosis of Hedgehog has opposite effects in flies and mice. Trends Cell Biol *18*, 360–363.

Bijlsma, M.F., Damhofer, H., and Roelink, H. (2012). Hedgehog-stimulated chemotaxis is mediated by smoothened located outside the primary cilium. Sci Signal *5*, ra60.

Bonneh-Barkay, D., Shlissel, M., Berman, B., Shaoul, E., Admon, A., Vlodavsky, I., Carey, D.J., Asundi, V.K., Reich-Slotky, R., and Ron, D. (1997). Identification of glypican as a dual modulator of the biological activity of fibroblast growth factors. J Biol Chem *272*, 12415–12421.

Bourikas, D., Pekarik, V., Baeriswyl, T., Grunditz, A., Sadhu, R., Nardó, M., and Stoeckli, E.T. (2005). Sonic hedgehog guides commissural axons along the longitudinal axis of the spinal cord. Nat Neurosci *8*, 297–304.

Briscoe, J., Chen, Y., Jessell, T.M., and Struhl, G. (2001). A hedgehog-insensitive form of patched provides evidence for direct long-range morphogen activity of sonic hedgehog in the neural tube. Mol Cell *7*, 1279–1291.

Buttitta, L., Mo, R., Hui, C.-C., and Fan, C.-M. (2003). Interplays of Gli2 and Gli3 and their requirement in mediating Shh-dependent sclerotome induction. Development *130*, 6233–6243.

Capurro, M.I., Xu, P., Shi, W., Li, F., Jia, A., and Filmus, J. (2008). Glypican-3 inhibits Hedgehog signaling during development by competing with patched for Hedgehog binding. Dev Cell *14*, 700–711.

Chan, J.A., Balasubramanian, S., Witt, R.M., Nazemi, K.J., Choi, Y., Pazyra-Murphy, M.F., Walsh, C.O., Thompson, M., and Segal, R.A. (2009). Proteoglycan interactions with Sonic Hedgehog specify mitogenic responses. Nat Neurosci *12*, 409–417.

Charron, F., Stein, E., Jeong, J., McMahon, A.P., and Tessier-Lavigne, M. (2003). The morphogen sonic hedgehog is an axonal chemoattractant that collaborates with netrin-1 in midline axon guidance. Cell *113*, 11–23.

Chédotal, A. (2011). Further tales of the midline. Curr Opin Neurobiol *21*, 68–75.

Chuang, P.-T., and McMahon, A.P. (1999). Vertebrate Hedgehog signalling modulated by induction of a Hedgehog-binding protein. Nature *397*, 617–621.

Condron, B. (2002). Gene expression is required for correct axon guidance. Curr Biol *12*, 1665–1669.

Das, R.M., van Hateren, N.J., Howell, G.R., Farrell, E.R., Bangs, F.K., Porteous, V.C., Manning, E.M., McGrew, M.J., Ohyama, K., Sacco, M.A., et al. (2006). A robust system for RNA interference in the chicken using a modified microRNA operon. Dev Biol *294*, 554–563.

Domanitskaya, E., Wacker, A., Mauti, O., Baeriswyl, T., Esteve, P., Bovolenta, P., and Stoeckli, E.T. (2010). Sonic hedgehog guides post-crossing commissural axons both directly and indirectly by regulating Wnt activity. J Neurosci *30*, 11167–11176.

Filmus, J., Capurro, M., and Rast, J. (2008). Glypicans. Genome Biol *9*, 224.

Goodrich, L.V., Johnson, R.L., Milenkovic, L., McMahon, J.A., and Scott, M.P. (1996). Conservation of the hedgehog/patched signaling pathway from flies to mice: induction of a mouse patched gene by Hedgehog. Genes Dev *10*, 301–312.

Hamburger, V., and Hamilton, H.L. (1951). A series of normal stages in the development of the chick embryo. J Morph *88*, 49–92.

Hu, H. (2001). Cell-surface heparan sulfate is involved in the repulsive guidance activities of Slit2 protein. Nat Neurosci *4*, 695–701.

Hynes, M., Ye, W., Wang, K., Stone, D., Murone, M., Sauvage, F.d., and Rosenthal, A. (2000). The seven-transmembrane receptor smoothened cell-autonomously induces multiple ventral cell types. Nat Neurosci *3*, 41–46.

Islam, S.M., Shinmyo, Y., Okafuji, T., Su, Y., Naser, I.B., Ahmed, G., Zhang, S., Chen, S., Ohta, K., Kiyonari, H., et al. (2009). Draxin, a repulsive guidance protein for spinal cord and forebrain commissures. Science *323*, 388–393.

Johnson, K.G., Ghose, A., Epstein, E., Lincecum, J., O'Connor, M.B., and van Vactor, D. (2004). Axonal heparan sulfate proteoglycans regulate the distribution and efficiency of the repellent slit during midline axon guidance. Curr Biol *14*, 499–504.

Joset, P., Wacker, A., Babey, R., Ingold, E.A., Andermatt, I., Stoeckli, E.T., and Gesemann, M. (2011). Rostral growth of commissural axons requires the cell adhesion molecule MDGA2. Neural Dev *6*, 22.

Kee, N., Wilson, N., Vries, M. de, Bradford, D., Key, B., and Cooper, H.M. (2008). Neogenin and RGMa control neural tube closure and neuroepithelial morphology by regulating cell polarity. J Neurosci *28*, 12643–12653.

Kennedy, T.E., Serafini, T., La Torre, J.R. de, and Tessier-Lavigne, M. (1994). Netrins are diffusible chemotropic factors for commissural axons in the embryonic spinal cord. Cell *78*, 425–435.

Kidd, T., Russell, C., Goodman, C.S., and Tear, G. (1999). Dosage-sensitive and complementary functions of roundabout and commissureless control axon crossing of the CNS midline. Neuron *20*, 25–33.

Kim, M.-S., Saunders, A.M., Hamaoka, B.Y., Beachy, P.A., and Leahy, D.J. (2011). Structure of the protein core of the glypican Dally-like and localization of a region important for hedgehog signaling. Proc Natl Acad Sci USA *108*, 13112–13117.

Li, F., Shi, W., Capurro, M., and Filmus, J. (2011). Glypican-5 stimulates rhabdomyosarcoma cell proliferation by activating Hedgehog signaling. J Cell Biol *192*, 691–704.

Long, H., Sabatier, C., Le Ma, Plump, A., Yuan, W., Ornitz, D.M., Tamada, A., Murakami, F., Goodman, C.S., and Tessier-Lavigne, M. (2004). Conserved roles for Slit and Robo proteins in midline commissural axon guidance. Neuron *42*, 213–223.

Lyuksyutova, A.I., Lu, C.-C., Milanesio, N., King, L.A., Guo, N., Wang, Y., Nathans, J., Tessier-Lavigne, M., and Zou, Y. (2003). Anterior-posterior guidance of commissural axons by Wnt-frizzled signaling. Science *302*, 1984–1988.

Mauti, O., Sadhu, R., Gemayel, J., Gesemann, M., and Stoeckli, E.T. (2006). Expression patterns of plexins and neuropilins are consistent with cooperative and separate functions during neural development. BMC Dev Biol *6*, 32.

Nawabi, H., Briançon-Marjollet, A., Clark, C., Sanyas, I., Takamatsu, H., Okuno, T., Kumanogoh, A., Bozon, M., Takeshima, K., Yoshida, Y., et al. (2010). A midline switch of receptor processing regulates commissural axon guidance in vertebrates. Genes Dev *24*, 396–410.

Niederkofler, V., Baeriswyl, T., Ott, R., and Stoeckli, E.T. (2010). Nectin-like molecules/SynCAMs are required for post-crossing commissural axon guidance. Development *137*, 427–435.

Okada, A., Charron, F., Morin, S., Shin, D.S., Wong, K., Fabre, P.J., Tessier-Lavigne, M., and McConnell, S.K. (2006). Boc is a receptor for sonic hedgehog in the guidance of commissural axons. Nature *444*, 369–373.

Oliver, T.G., Grasfeder, L.L., Carroll, A.L., Kaiser, C., Gillingham, C.L., Lin, S.M., Wickramasinghe, R., Scott, M.P., and Wechsler-Reya, R.J. (2003). Transcriptional profiling of the Sonic hedgehog response: a critical role for N-myc in proliferation of neuronal precursors. Proc Natl Acad Sci USA *100*, 7331–7336.

Parra, L.M., and Zou, Y. (2010). Sonic hedgehog induces response of commissural axons to Semaphorin repulsion during midline crossing. Nat Neurosci *13*, 29–35.

Parsons, B.D., Schindler, A., Evans, D.H., Foley, E., and Freitag, M. (2009). A direct phenotypic comparison of siRNA pools and multiple individual duplexes in a functional assay. PLoS One *4*, e8471.

Rawson, J.M., Dimitroff, B., Johnson, K.G., Rawson, J.M., Ge, X., van Vactor, D., and Selleck, S.B. (2005). The heparan sulfate proteoglycans Dally-like and Syndecan have distinct functions in axon guidance and visual-system assembly in Drosophila. Curr Biol *15*, 833–838.

Rikin, A., Rosenfeld, G.E., McCartin, K., and Evans, T. (2010). A reverse genetic approach to test functional redundancy during embryogenesis. J Vis Exp *42*, e2020

Ronca, F., Andersen, J.S., Paech, V., and Margolis, R.U. (2001). Characterization of Slit protein interactions with glypican-1. J Biol Chem *276*, 29141–29147.

Sanchez-Camacho, C., and Bovolenta, P. (2009). Emerging mechanisms in morphogen-mediated axon guidance. Bioessays *31*, 1013–1025.

Smart, A.D., Course, M.M., Rawson, J., Selleck, S., van Vactor, D., and Johnson, K.G. (2011). Heparan sulfate proteoglycan specificity during axon pathway formation in the Drosophila embryo. Devel Neurobio *71*, 608–618.

Stoeckli, E.T., and Landmesser, L.T. (1995). Axonin-1, Nr-CAM, and Ng-CAM play different roles in the in vivo guidance of chick commissural neurons. Neuron *14*, 1165–1179.

Tenzen, T., Allen, B.L., Cole, F., Kang, J.-S., Krauss, R.S., and McMahon, A.P. (2006). The cell surface membrane proteins Cdo and Boc are components and targets of the Hedgehog signaling pathway and feedback network in mice. Dev Cell *10*, 647–656.

Williams, E.H., Pappano, W.N., Saunders, A.M., Kim, M.-S., Leahy, D.J., and Beachy, P.A. (2010). Dally-like core protein and its mammalian homologues mediate stimulatory and inhibitory effects on Hedgehog signal response. Proc Natl Acad Sci USA *107*, 5869–5874.

Wilson, N.H., and Key, B. (2006). Neogenin interacts with RGMa and netrin-1 to guide axons within the embryonic vertebrate forebrain. Dev Biol *296*, 485–498.

Wilson, N.H., and Stoeckli, E.T. (2011). Cell type specific, traceable gene silencing for functional gene analysis during vertebrate neural development. Nucleic Acids Res *39*, e133.

Wilson, N.H., and Stoeckli, E.T. (2012) *In ovo* electroporation of miRNA-based plasmids in the developing neural tube and assessment of phenotypes by DiI injection in open-book preparations. J Vis Exp *68*, e4384.

Yam, P.T., Langlois, S.D., Morin, S., and Charron, F. (2009). Sonic hedgehog guides axons through a noncanonical, Src-family-kinase-dependent signaling pathway. Neuron *62*, 349–362.

Yam, P.T., Kent, C.B., Morin, S., Farmer, W.T., Alchini, R., Lepelletier, L., Colman, D.R., Tessier-Lavigne, M., Fournier, A.E., and Charron, F. (2012). 14-3-3 proteins regulate a cell-intrinsic switch from sonic hedgehog-mediated commissural axon attraction to repulsion after midline crossing. Neuron *76*, 735–749.

Yan, D., Wu, Y., Yang, Y., Belenkaya, T.Y., Tang, X., and Lin, X. (2010). The cell-surface proteins Dally-like and Ihog differentially regulate Hedgehog signaling strength and range during development. Development *137*, 2033–2044.

Yang, L., Garbe, D.S., and Bashaw, G.J. (2009). A frazzled/DCC-dependent transcriptional switch regulates midline axon guidance. Science *324*, 944–947.

Zhang, X., Liu, C., Nestor, K.E., McFarland, D.C., and Velleman, S.G. (2007). The effect of glypican-1 glycosaminoglycan chains on turkey myogenic satellite cell proliferation, differentiation, and fibroblast growth factor 2 responsiveness. Poult Sci *86*, 2020–2028.

Zheng, L. (2004). An efficient one-step site-directed and site-saturation mutagenesis protocol. Nucleic Acids Res *32*, e115.

Zou, Y., Stoeckli, E., Chen, H., and Tessier-Lavigne, M. (2000). Squeezing axons out of the gray matter: a role for slit and semaphorin proteins from midline and ventral spinal cord. Cell *102*, 363–375.

Figure Legends

Figure 1. Loss of GPC1 causes axon guidance defects at the neural tube midline.

(A) *In situ* hybridization for *GPC1* localizes expression to the floorplate (arrowhead), motor neurons (circles), dorsal root ganglia (asterisks) and commissural neurons (arrow) at the stages indicated. For hybridization with the sense probe, see Figure S1. Dorsal is up. (B) Dissociated commissural neurons obtained from HH25-26 chicken embryos were immunolabeled for Cntn2 and GPC1. GPC1 decorated the cell bodies (*), axons and growth cones (arrowheads) of the neurons identified by Cntn2. (C) Schematic of the miRNA construct used for unilateral knockdown (C') of GPC1. (D) In control embryos, dI1 axons crossed the floorplate (fp) and turned rostrally along the contralateral floorplate border (yellow arrowheads). R, rostral; C, caudal. (E-G) Pathfinding errors observed after downregulation of GPC1 were stalling in the floorplate (arrows in E); post-crossing errors consisting of axons failing to turn (asterisks in E-G), or axons turning caudally (open arrows in F, G); and occasional ipsilateral errors which mainly included axons stalling at the floorplate entry site, or in very rare cases axons extending along the ipsilateral floorplate border (arrowheads).

(H) Quantification of guidance defects. n=number of DiI injection sites. * $p<0.05$; *** $p<0.0001$; Fisher exact test. (I) GPC∆miR, a knockdown-resistant form of GPC1, was obtained by the exchange of 5 nucleotides (red) in the target site of mi7GPC1 (underlined). Boxes indicate regions important for miRNA targeting and cleavage. (J) Constructs co-electroporated in the rescue experiments. In contrast to the knockdown condition (K-K'), most axons projected normally after the rescue (L-L'). (M) Quantification of rescue experiments. * $p<0.05$; *** $p<0.0001$; ns, not significant; Fisher exact test. Bar, 50 µm, except F, where bar is 25 µm.

See also Figures S1, S2, S3, S4, S6 and Table S1.

Figure 2. Cell type-specific knockdown of GPC1 demonstrates its requirement in dI1 axons.

(A) Schematic of the bilaterally electroporated miR construct to drive floorplate-specific knockdown (A'). Hoxa1, enhancer element III of mouse *Hoxa1*; TATA, minimal TATA box promoter. (B) Downregulation of GPC1 in the floorplate with *Hox-EGFP-mi7GPC1* did not change axon projections (yellow arrowheads) in comparison to electroporation with *Hox-EGFP-mi1Luc* (C) or untreated embryos. (D) Quantification after floorplate-specific knockdown of GPC1. ns, not significant; Fisher exact test. (E) Schematic of the dI1 neuron-specific (E') knockdown construct. Math1, enhancer of mouse *Math1*; βglob, basal *β-globin* promoter; F, farnesylation signal. (F) Examples of pathfinding errors after downregulation of GPC1 specifically in dI1 neurons by electroporation of *Math1-EGFPF-mi7GPC1*: floorplate stalling (arrows), and post-crossing errors (no turning, asterisks; caudal turning, open arrows). The majority of aberrant axons expressed mi7GPC1 (axons appear yellow in merged images on right). (G) Electroporation of a control construct specifically in dI1 neurons (*Math1-EGFPF-mi1Luc*) did not interfere with normal trajectories (yellow arrowheads). (H) Quantification of axon trajectories after silencing GPC1 in commissural neurons. * $p<0.05$, ** $p<0.001$, *** $p<0.0001$, Fisher exact test; n=number of DiI sites. Bar: 50 µm.

See also Figures S2 and S3.

Figure 3. GPC1 and Shh interact in commissural axon guidance.

(A) Schematics of the miR constructs co-electroporated to drive simultaneous knockdown of distinct genes in dI1 neurons and floorplate. (A') Representative spinal cord cross-section,

with EBFP2 (blue) in the floorplate and EGFP (green) in commissural axons. (B-E) Examples of axon pathfinding phenotypes in open-book preparations. Control embryos co-expressing the control construct mi1Luc in both floorplate and commissural neurons displayed normal pathfinding (B), as did embryos treated with low concentrations of miGPC1 (C) or miShh (D) (yellow arrowheads in B-D). However, the co-electroporation of these low amounts of miRNAs, targeting GPC1 in axons and Shh in the floorplate (E), prevented many post-crossing commissural axons from turning into the longitudinal axis (asterisks). Bar: 50 µm. (F) Quantification of combinatorial knockdowns. *$p<0.05$, Fisher exact test. See also Table S2. (G) GPC1 and Shh also interact biochemically as shown by co-immunoprecipitation. HEK293T cells were transfected with *GPC1-HA* and/or *Shh-FLAG* expression vectors as indicated, and cell lysates were analyzed by Western blotting with the antibodies indicated on the right. Upper panels show GPC1 and Shh in the cell lysates used for co-immunoprecipitation. GPC1 was detected as a major band at ~70 kDa. Shh was detected as a full-length ~45 kDa protein, and as a cleaved N-terminal (secreted) fragment of ~20kDa. Lower panel shows bands obtained with the anti-GPC1 antibody after immunoprecipitation with anti-FLAG antibodies, indicating that GPC1 and Shh co-precipitated.
See also Tables S1, S2, and S3.

Figure 4. GPC1 is required cell-autonomously for *Hhip* mRNA expression in dI1 neurons.

(A) *Hhip* mRNA expression in the dorsal spinal cord was lost (arrows) on the electroporated side (GFP, insets) after unilaterally knocking down GPC1 with mi7GPC1. Knockdown of GPC1 did not affect *Hhip* expression in the medial spinal cord (boxed area). (B) Expression of

mi2Luc had no effect on *Hhip* expression. (C-F) Rescue experiments, as shown in Figure 1, restored *Hhip* expression (arrowheads in E). In untreated control embryos (C) symmetrical *Hhip* expression in the dorsal spinal cord was seen in 86% of all sections. After downregulation of GPC1, symmetrical *Hhip* expression was seen in only 37% of the sections (D). Dorsal *Hhip* expression was restored by co-electroporation of a knockdown-resistant version of *GPC1* (*GPC1*Δ*miR*; E). Rescue with an unglycanated form of GPC1, GPC1ΔmiRΔGAG, only partially restored *Hhip* expression (open arrows in F). (G) Quantification of the effects of GPC1 knockdown and rescue experiments on *Hhip* expression in the dorsal and medial spinal cord based on pixel intensity (PI) ratios (see text for details). Data is presented as mean +/- SEM. Average PI^{elect}:$PI^{control}$ in the medial spinal cord was always close to 1, indicating symmetrical staining, whereas dorsal *Hhip* expression was variable. To assess the 'symmetry' of *Hhip* expression in each treatment, the dorsal ratios were first subjected to a single sample t-test against a hypothetical mean of 1 (shown in green). To assess the ability of the different rescue treatments to restore symmetry, the dorsal ratios were subjected to two-sample t-tests between the groups (shown in black). *$p<0.05$; *** $p<0.0001$; ns, not significant. (H) Quantification of axon guidance phenotypes in Hhip rescue experiments, where Hhip was expressed ectopically in embryos lacking GPC1. *$p<0.05$, Fisher exact test. Compare to Figure 1M. (I) Example of normal axon projections (yellow arrowheads) in an embryo co-electroporated with *pMES-Hhip* and *βactin-EBFP2-mi7GPC1*. (J) Loss of *Hhip* mRNA expression in the dorsal spinal cord (arrows) after dI1-specific knockdown of GPC1. Bar: 50 µm. %, proportion of sections displaying symmetrical *Hhip* expression in the dorsal spinal cord.

See also Figures S3, S4, S5, and S6.

Figure 5. The canonical Shh pathway is activated downstream of GPC1 to induce *Hhip* in commissural neurons.

(A) Analysis of *Hhip* expression following stimulation of the canonical Shh signaling pathway by electroporation of *Gli1*, *Gli2*, or *Smo-M2* constructs (right side, indicated by GFP in insets). Note that misexpression of Gli1 and Gli2 caused additional gross developmental abnormalities. (B) *Hhip* expression is lost specifically in the dorsal spinal cord (arrows) following electroporation of a construct encoding *Ptc∆loop2* (right side), a dominant repressor of Smo that is unable to bind Shh. Symmetrical *Hhip* expression in the dorsal spinal cord was only found in 7% of the sections. (C) Co-immunoprecipitations of mutant forms of GPC1 and Shh. HEK293T cells were transfected with myc-tagged *GPC1* constructs and/or *Shh-FLAG* expression vectors as indicated, and cell lysates were analyzed by Western blotting with the antibodies indicated on the right. Lower panel shows bands obtained with the anti-GPC1 antibody when immunoprecipitation (IP) was carried out with anti-FLAG gel, indicating that GPC1 and GPC1∆GAG co-precipitated with Shh, but GPC1∆GAG∆Shh did not. GAPDH was used as a loading control. (D) *Hhip* expression could not be rescued with GPC1∆miR∆GAG∆Shh, a GPC1 form unable to bind Shh (arrows). Only 24% of all sections exhibited symmetrical *Hhip* expression in the dorsal spinal cord. Compare to Figure 4C-F. (E) Quantification of the effects of Ptc∆loop2 expression and GPC1∆miR∆GAG∆Shh rescue experiments on *Hhip* expression in the dorsal and medial spinal cord. Data is presented as mean +/- SEM. To assess the 'symmetry' of *Hhip* expression in each treatment, the dorsal pixel intensity (PI) ratios were first subjected to a single sample t-test against a hypothetical mean of 1 (shown in green). To assess the ability of the GPC1∆miR∆GAG∆Shh to restore

symmetry following GPC1 knockdown, the dorsal ratios were subjected to two-sample t-tests between the relevant groups (shown in black). *** p<0.0001; ns, not significant. Bar, 50 µm. See also Figures S4, S5, and S6.

Figure 6. Expression of GPC1∆miR∆GAG∆Shh cannot rescue the axon guidance defects induced by loss of GPC1.

Rescue experiments were carried out as in Figure1. Embryos in the different groups (control, knockdown, or ∆Shh rescue) were co-electroporated with *βactin-EBFP2-miR* (encoding *mi2Luc* or *mi7GPC1*; blue) and *pMES* constructs (with or without *GPC1∆miR∆GAG∆Shh*; green), as indicated in panel A. (A) Quantification of rescue experiments. * p<0.05; *** p<0.0001; ns, not significant; Fisher exact test. Compare to Figure 1M and Figure 4H. (B-B') Normal axonal projections at a DiI-injection site of a control embryo: Axons cross the floorplate (indicated by dashed lines), then turn and extend rostrally (yellow arrowheads). (C-C') Example of abnormal axonal projections following GPC1 knockdown: Axons fail to turn into the longitudinal axis (asterisks) after crossing the floorplate. See also Figure 1K-K'. (D-E') Examples of abnormal axon projections following the attempted rescue of the GPC1 knockdown phenotype with GPC1∆miR∆GAG∆Shh, a mutant form of GPC1 that is incapable of binding Shh: commissural axons stall in the floorplate (arrows) and/or fail to turn into the longitudinal axis after crossing the floorplate (asterisks). Bar, 50 µm.

Figure 7. GPC1 promotes canonical Shh signaling *in vivo*, but is not an obligate co-factor in all Shh-responsive cells.

(A-B) GPC1 was knocked down unilaterally by electroporation of *βactin-hrGFPII-mi7GPC1* (green, insets) and *in situ* hybridization was performed as indicated. There were no differences in the expression of the Shh transcriptional targets *Boc, Ptc1, Sfrp1* between control and electroporated sides of the spinal cord (A). Both *Ptc1* and *Sfrp1* have been identified as positive transcriptional targets of canonical Shh signaling, whereas *Boc* is negatively regulated by Shh. No changes were found also for *Fzd3* (B), a Wnt receptor that transduces the attractive effects of Wnt in post-crossing axons, a guidance system that works in collaboration with Shh to drive axons rostrally. (C) Quantification of the effects of GPC1 overexpression on Shh target genes. n=number of sections. (D) Sections from embryos in which GPC1 was overexpressed by electroporation of *pMES-GPC1* (green, insets), showing ectopic expression of Shh target genes (arrowheads). Bar, 100 µm.
See also Figure S6.

Figure 8. Model for the GPC1-dependent transcriptional switch of axonal response to Shh.

In pre-crossing axons (green arrows), Src Family Kinases (SFK) mediate attraction towards Shh in the floorplate in a transcription-independent manner (Charron et al., 2003; Okada et al., 2006; Yam et al., 2009). In parallel, Shh interacting with GPC1 and involving Ptc induces *Hhip* transcription (blue arrows) once axons have reached the midline (this study). Thus, post-crossing axons express Hhip, which mediates a repulsive Shh signal (red arrows) (this study; Bourikas et al., 2005) and guides axons along the caudal^{high}-rostal^{low} gradient of Shh in the floorplate (Bourikas et al., 2005). GPC1 could also facilitate the assembly of a Hhip co-receptor complex.

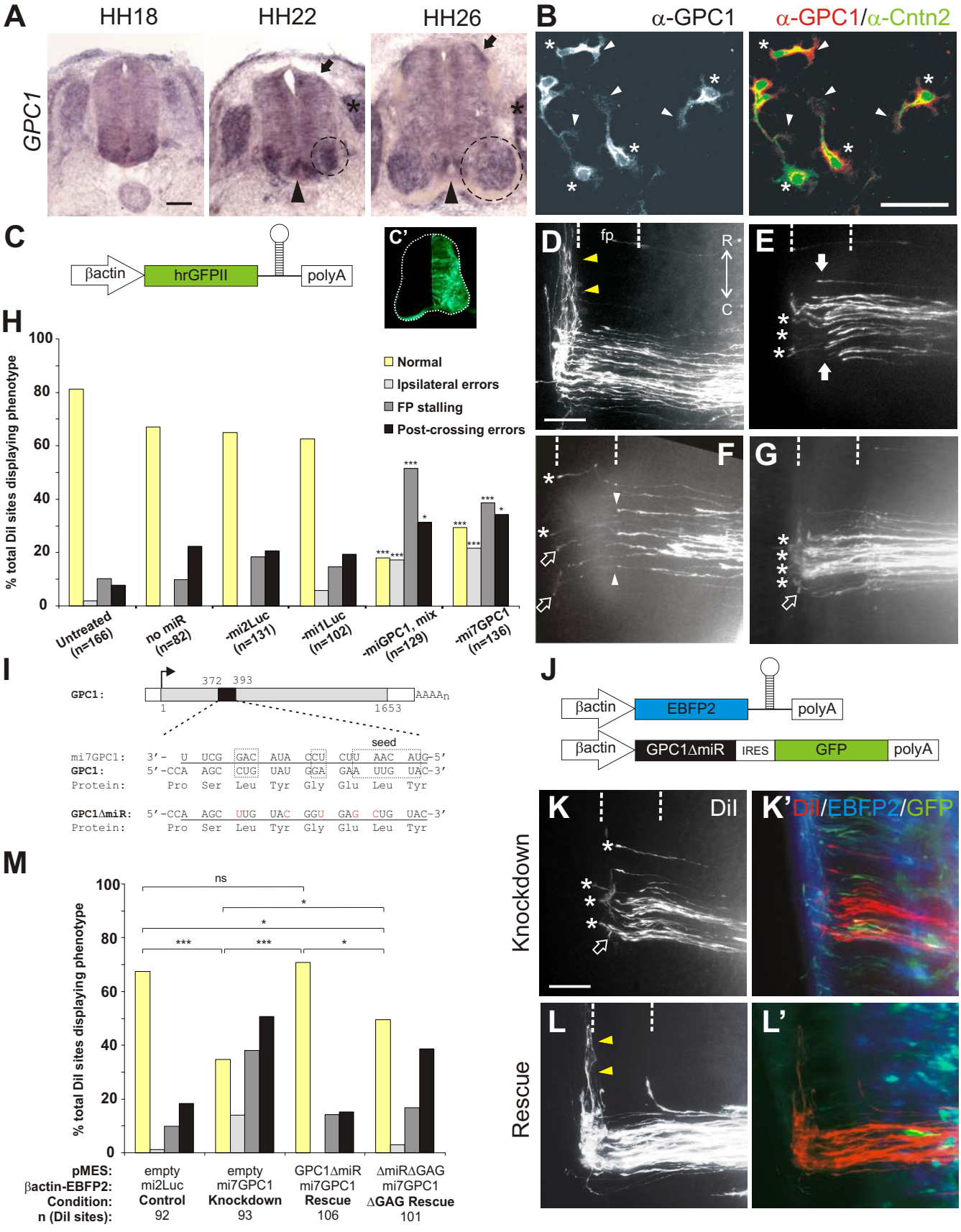
A
HH18
HH22
HH26
GPC1
B
α-GPC1
α-GPC1/α-Cntn2
C
βactin
hrGFPII
polyA
C'
D
fp
R
C
E
F
G
H
% total DiI sites displaying phenotype
Normal
Ipsilateral errors
FP stalling
Post-crossing errors
Untreated (n=166)
no miR (n=82)
-mi2Luc (n=131)
-mi1Luc (n=102)
-miGPC1, mix (n=129)
-mi7GPC1 (n=136)
I
GPC1:
372 393
AAAAn
1
1653
seed
mi7GPC1: 3'- U UCG GAC AUA CCU CUU AAC AUG-5'
GPC1: 5'-CCA AGC CUG UAU GGA GAA UUG UAC-3'
Protein: Pro Ser Leu Tyr Gly Glu Leu Tyr
GPC1ΔmiR: 5'-CCA AGC UUG UAC GGU GAG CUG UAC-3'
Protein: Pro Ser Leu Tyr Gly Glu Leu Tyr
J
βactin
EBFP2
polyA
βactin
GPC1ΔmiR
IRES
GFP
polyA
K
DiI
K'DiI/EBFP2/GFP
Knockdown
L
L'
Rescue
M
% total DiI sites displaying phenotype
ns
pMES:
βactin-EBFP2:
Condition:
n (DiI sites):
empty
mi2Luc
Control
92
empty
mi7GPC1
Knockdown
93
GPC1ΔmiR
mi7GPC1
Rescue
106
ΔmiRΔGAG
mi7GPC1
ΔGAG Rescue
101

Fig. 1

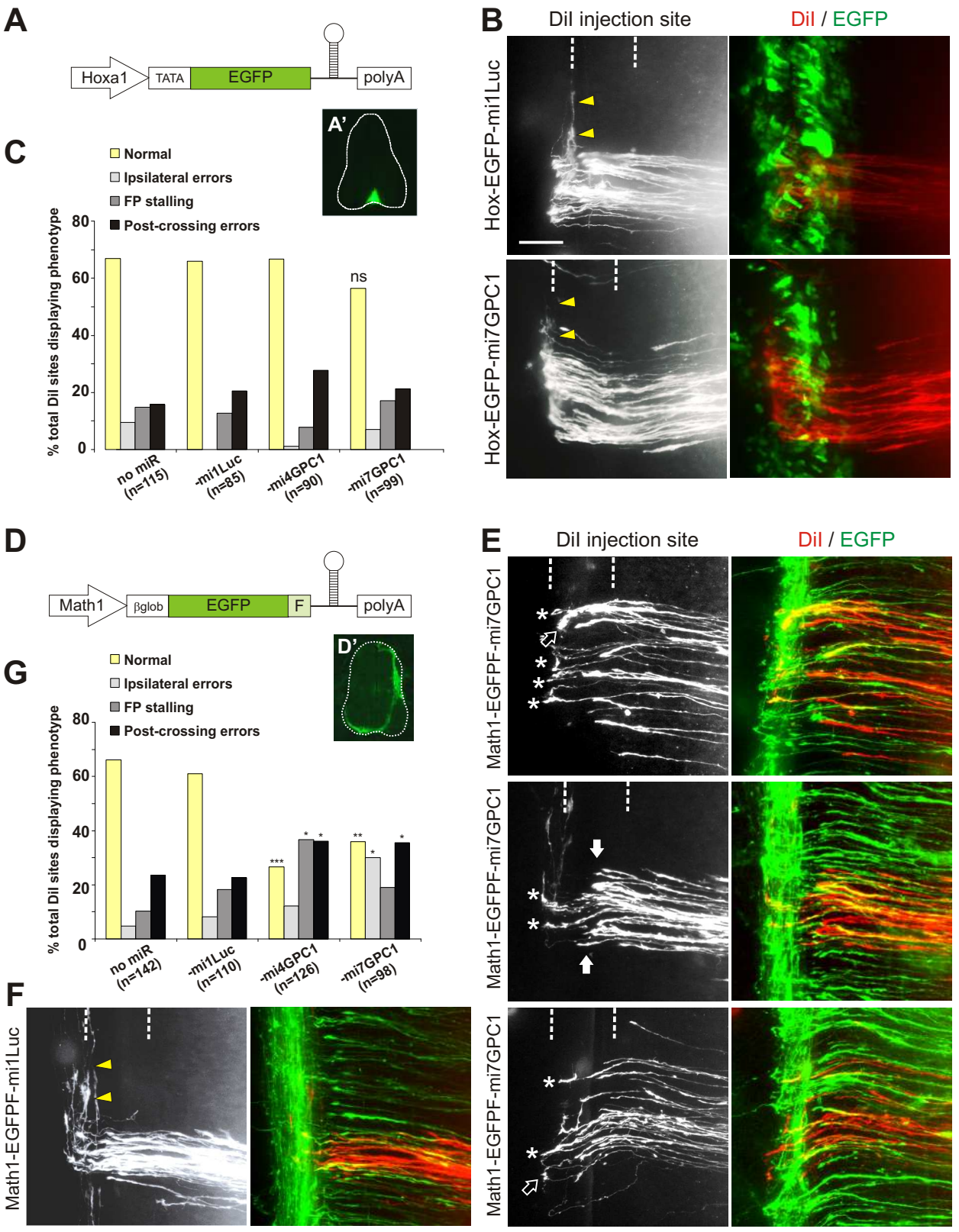
A
Hoxa1
TATA
EGFP
polyA
A'
B
DiI injection site
DiI / EGFP
Hox-EGFP-mi1Luc
Hox-EGFP-mi7GPC1
C
Normal
Ipsilateral errors
FP stalling
Post-crossing errors
% total DiI sites displaying phenotype
80
60
40
20
0
ns
no miR (n=115)
-mi1Luc (n=85)
-mi4GPC1 (n=90)
-mi7GPC1 (n=99)
D
Math1
βglob
EGFP
F
polyA
D'
E
DiI injection site
DiI / EGFP
Math1-EGFPF-mi7GPC1
Math1-EGFPF-mi7GPC1
Math1-EGFPF-mi7GPC1
G
Normal
Ipsilateral errors
FP stalling
Post-crossing errors
% total DiI sites displaying phenotype
80
60
40
20
0
***
**
*
no miR (n=142)
-mi1Luc (n=110)
-mi4GPC1 (n=126)
-mi7GPC1 (n=98)
F
Math1-EGFPF-mi1Luc

Fig. 2

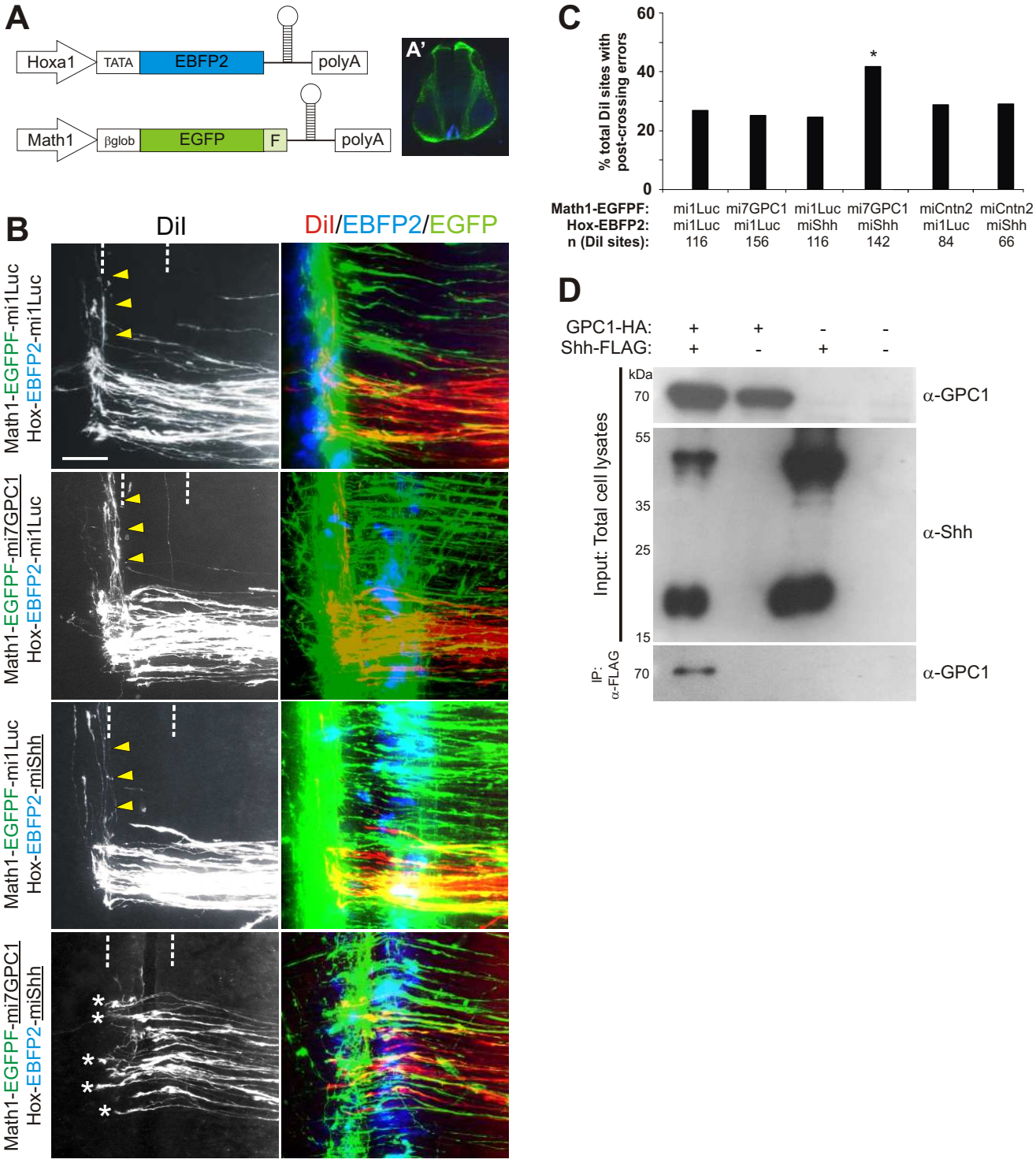
A
Hoxa1
TATA
EBFP2
polyA
Math1
βglob
EGFP
F
polyA
A'
B
DiI
DiI/EBFP2/EGFP
Math1-EGFPF-mi1Luc
Hox-EBFP2-mi1Luc
Math1-EGFPF-mi7GPC1
Hox-EBFP2-mi1Luc
Math1-EGFPF-mi1Luc
Hox-EBFP2-miShh
Math1-EGFPF-mi7GPC1
Hox-EBFP2-miShh
C
% total DiI sites with post-crossing errors
60
40
20
0
*
Math1-EGFPF:
Hox-EBFP2:
n (DiI sites):
mi1Luc mi1Luc 116
mi7GPC1 mi1Luc 156
mi1Luc miShh 116
mi7GPC1 miShh 142
miCntn2 mi1Luc 84
miCntn2 miShh 66
D
GPC1-HA: + + - -
Shh-FLAG: + - + -
kDa
70
55
35
25
15
Input: Total cell lysates
α-GPC1
α-Shh
IP: α-FLAG
70
α-GPC1

Fig. 3

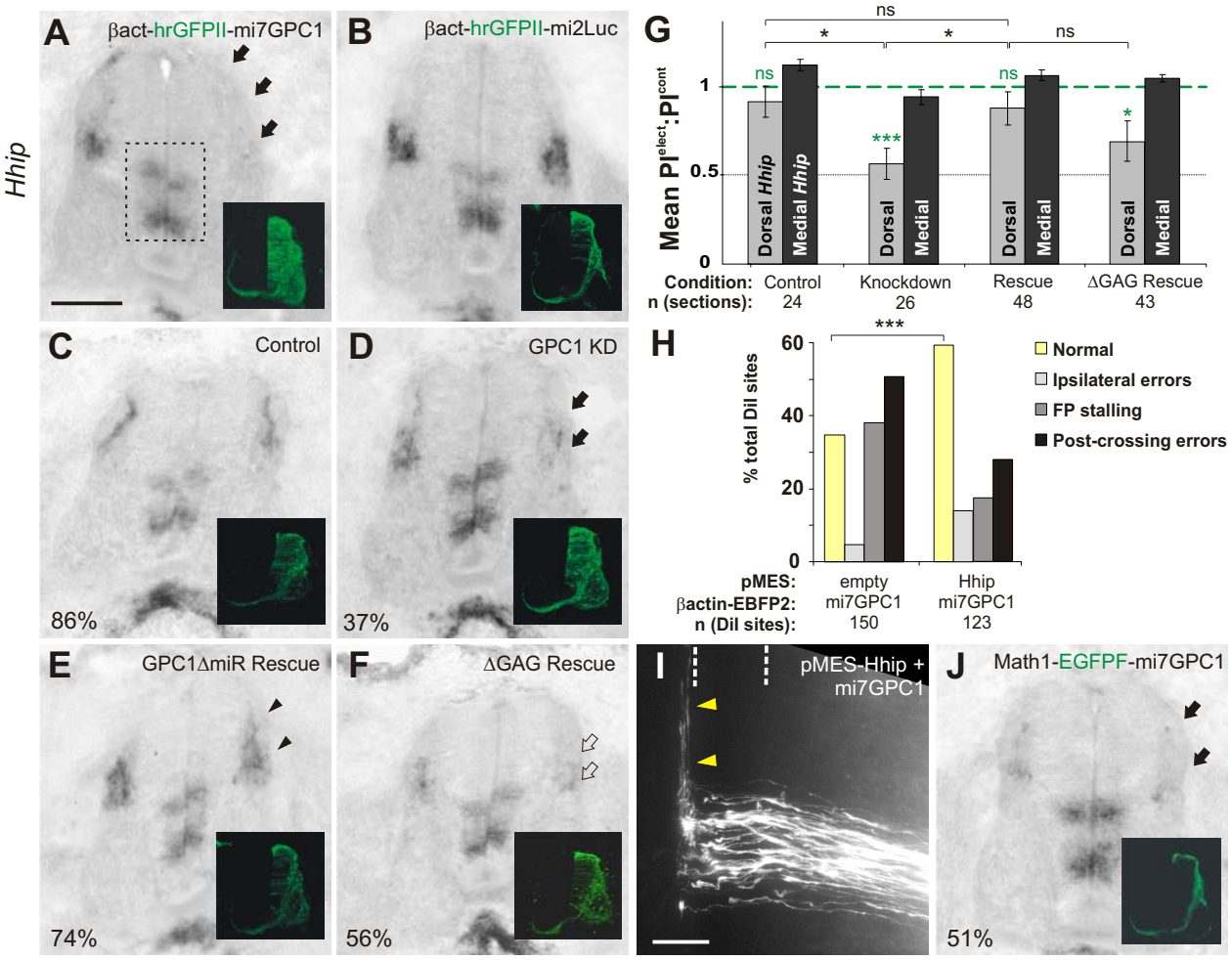
Hhip
A
βact-hrGFPII-mi7GPC1
B
βact-hrGFPII-mi2Luc
C
Control
86%
D
GPC1 KD
37%
E
GPC1ΔmiR Rescue
74%
F
ΔGAG Rescue
56%
G
Mean PI^elect.:PI^cont
ns
*
*
ns
ns
ns
***
*
1
0.5
0
Dorsal Hhip
Medial Hhip
Dorsal
Medial
Dorsal
Medial
Dorsal
Medial
Condition: Control Knockdown Rescue ΔGAG Rescue
n (sections): 24 26 48 43
H
***
% total DiI sites
60
40
20
0
Normal
Ipsilateral errors
FP stalling
Post-crossing errors
pMES: empty Hhip
βactin-EBFP2: mi7GPC1 mi7GPC1
n (DiI sites): 150 123
I
pMES-Hhip +
mi7GPC1
J
Math1-EGFPF-mi7GPC1
51%

Fig. 4

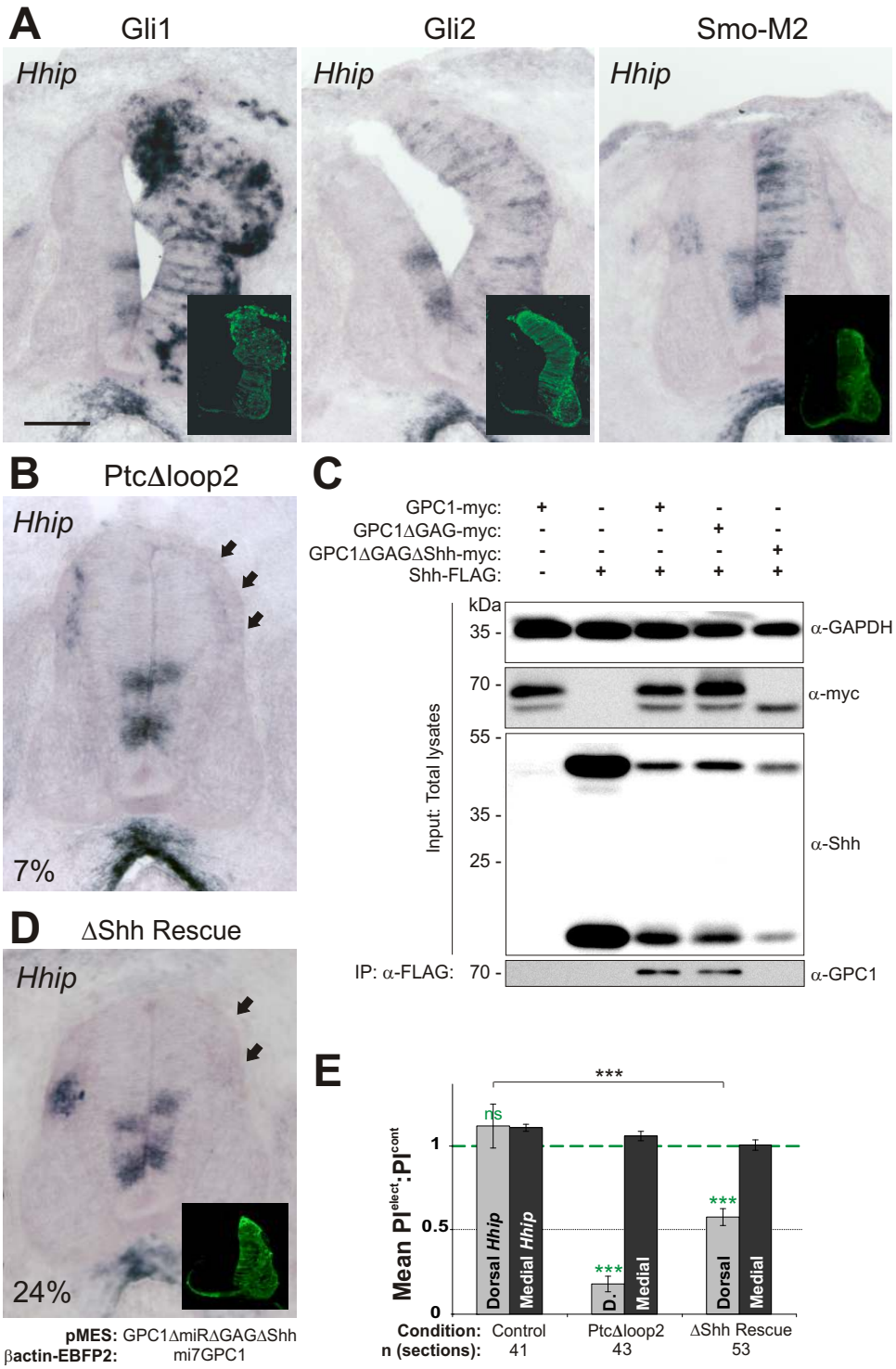
A
Gli1
Gli2
Smo-M2
Hhip
Hhip
Hhip
B
PtcΔloop2
Hhip
7%
C
GPC1-myc: + - + - -
GPC1ΔGAG-myc: - - - + -
GPC1ΔGAGΔShh-myc: - - - - +
Shh-FLAG: - + + + +
kDa
35 -
70 -
55 -
35 -
25 -
Input: Total lysates
α-GAPDH
α-myc
α-Shh
IP: α-FLAG: 70 -
α-GPC1
D
ΔShh Rescue
Hhip
24%
pMES: GPC1ΔmiRΔGAGΔShh
βactin-EBFP2: mi7GPC1
E
Mean PI elect.:PI cont
***
ns
1
0.5
0
***
***
Dorsal Hhip
Medial Hhip
D.
Medial
Dorsal
Medial
Condition: Control PtcΔloop2 ΔShh Rescue
n (sections): 41 43 53

Fig. 5

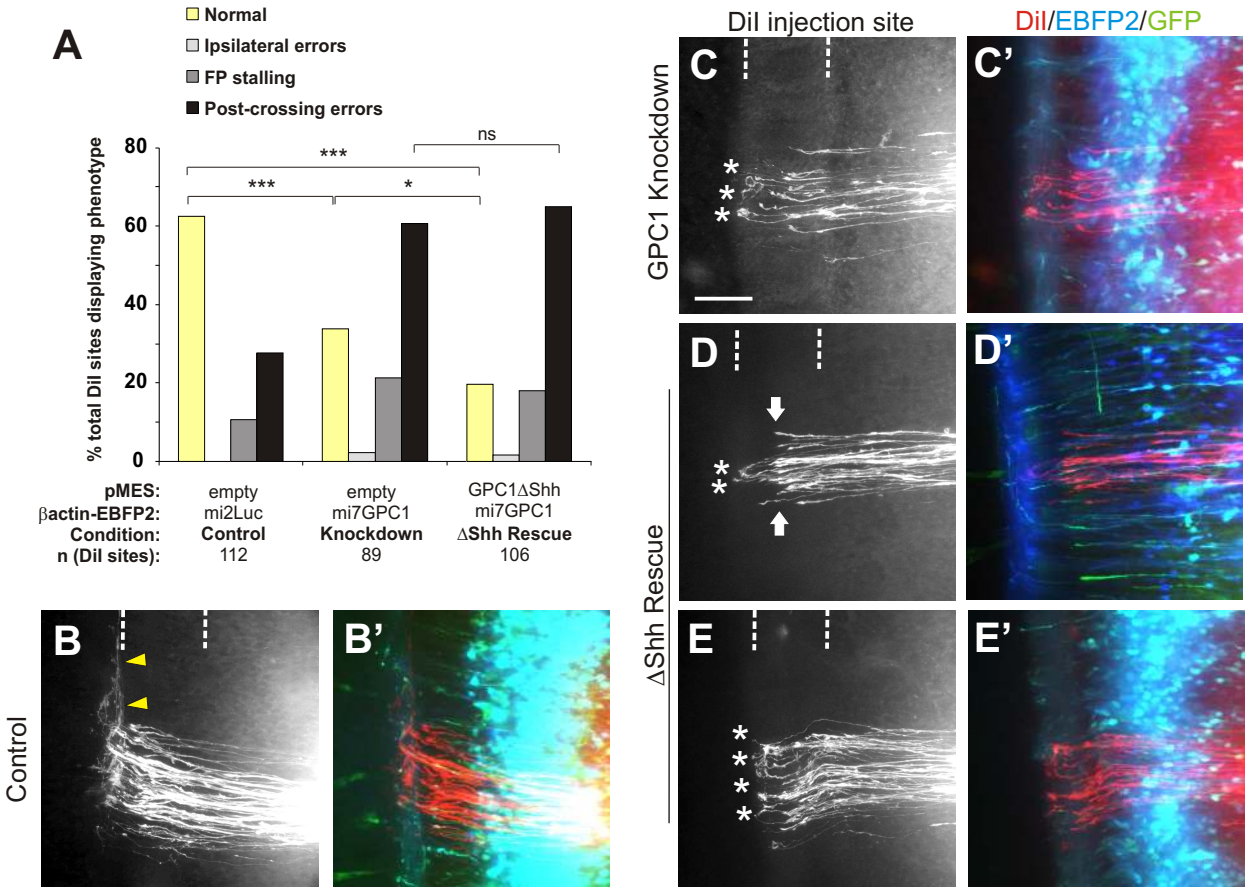
A
Normal
Ipsilateral errors
FP stalling
Post-crossing errors
% total DiI sites displaying phenotype
80
60
40
20
0
***
***
*
ns
pMES:
βactin-EBFP2:
Condition:
n (DiI sites):
empty
mi2Luc
Control
112
empty
mi7GPC1
Knockdown
89
GPC1ΔShh
mi7GPC1
ΔShh Rescue
106
DiI injection site
DiI/EBFP2/GFP
GPC1 Knockdown
ΔShh Rescue
Control
B
B'
C
C'
D
D'
E
E'

Fig. 6

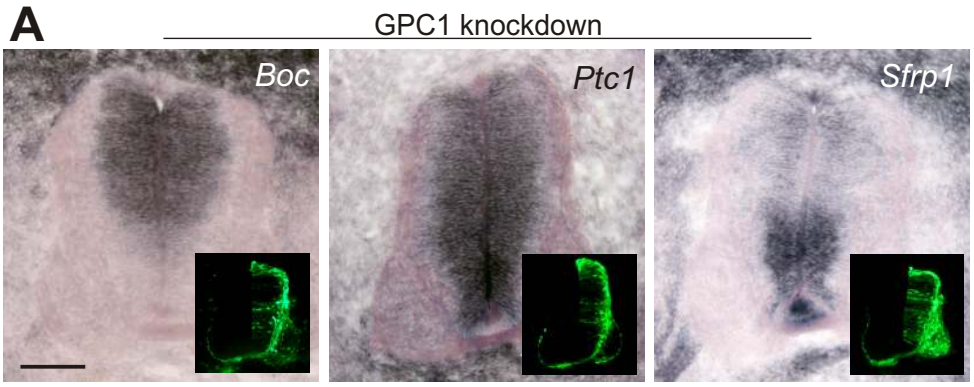

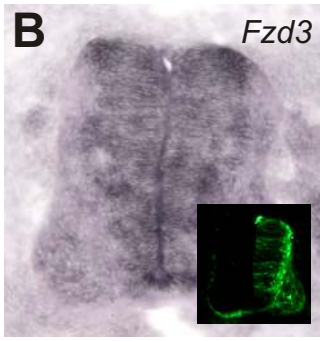

C

Phenotypes after GPC1 overexpression

Probe	# embryos with ectopic expression	% total sections with ectopic expression (n)
Ptc1	9/11	38% (69)
Sfrp1	11/11	39% (69)
Hhip	10/12	47% (76)

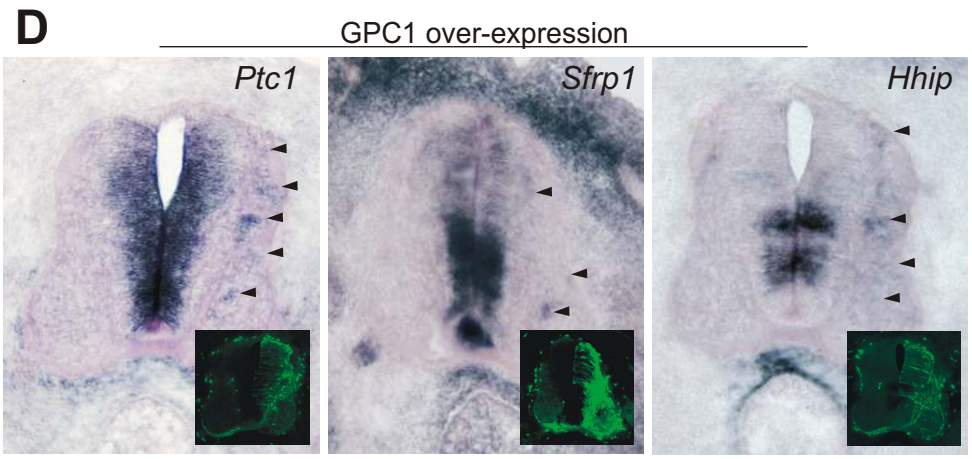

Fig. 7

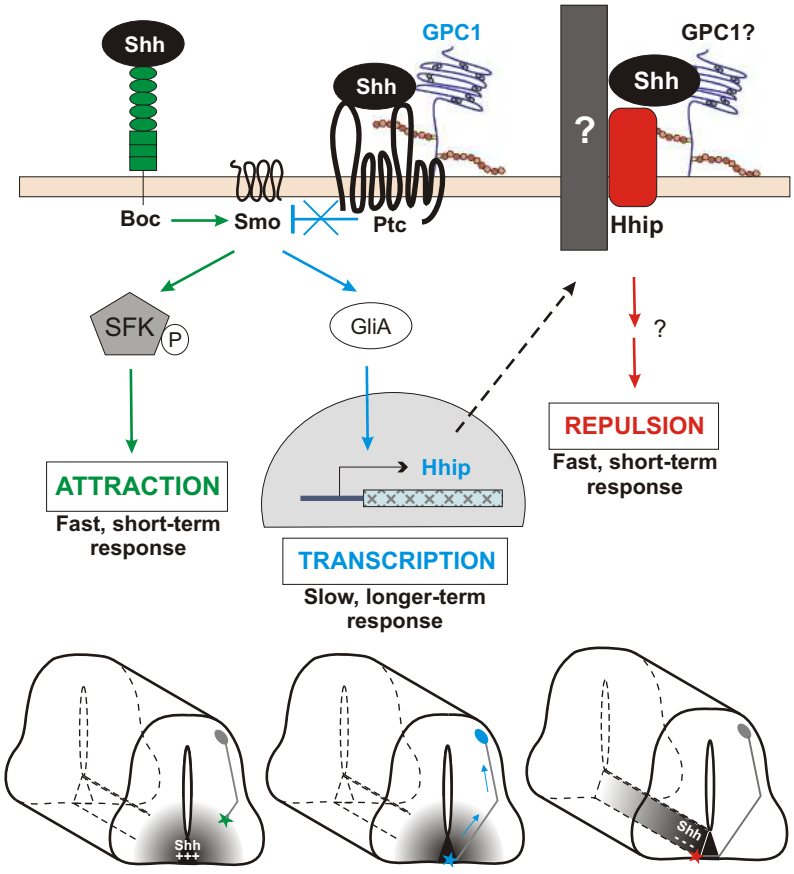
Shh
GPC1
Shh
GPC1?
Shh
?
Boc
Smo
Ptc
Hhip
SFK
P
GliA
?
ATTRACTION
Fast, short-term response
Hhip
REPULSION
Fast, short-term response
TRANSCRIPTION
Slow, longer-term response
Shh +++
Shh

Fig. 8

Neuron, Volume *79*

Supplemental Information

Sonic Hedgehog Regulates Its Own Receptor on Postcrossing Commissural Axons in a Glypican1-Dependent Manner

Nicole H. Wilson and Esther T. Stoeckli

Inventory of Supplemental Information

Supplemental Figures

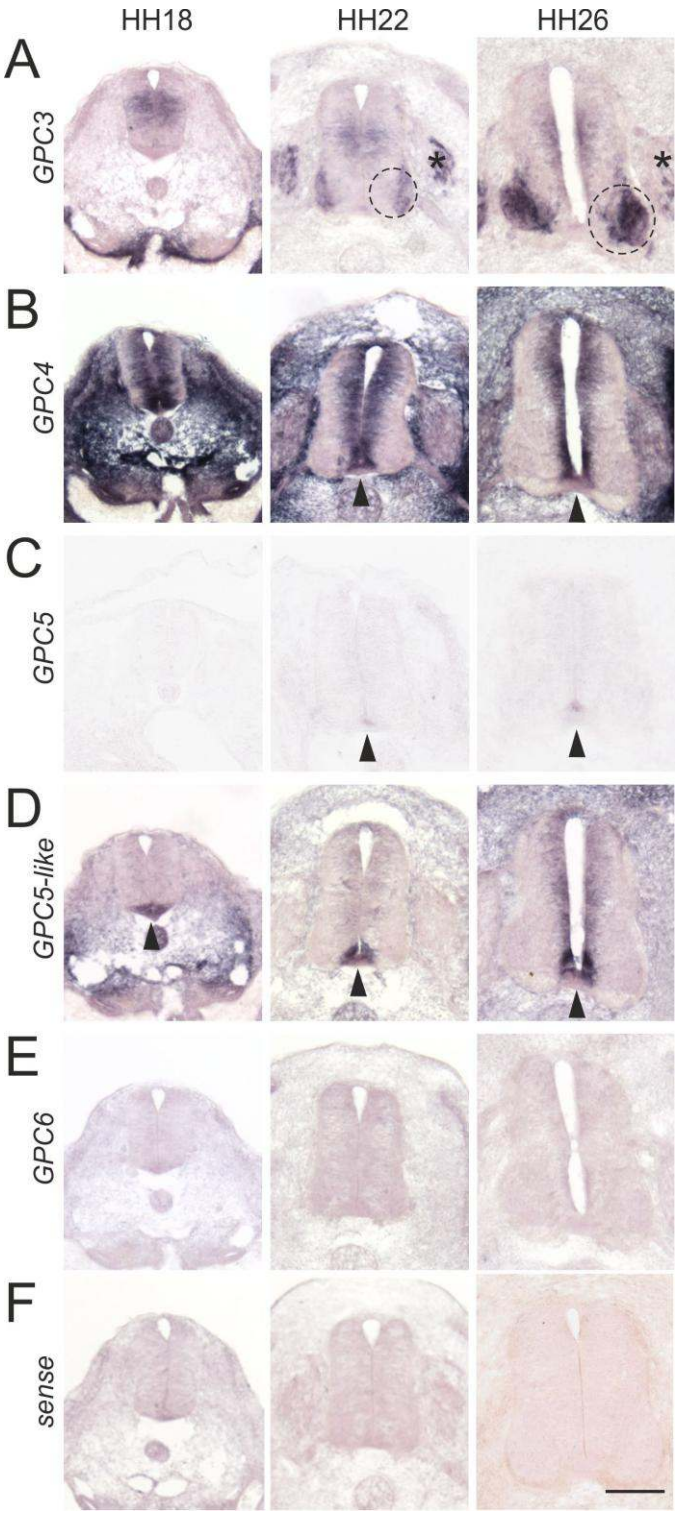

Figure S1. Expression patterns of Glypicans in the developing chicken neural tube. Related to Figure 1.

In situ hybridization for *GPC3* (A), *GPC4* (B), *GPC5* (C), *GPC5-like* (D), and *GPC6* (E) was performed on cross sections of chicken spinal cords at the indicated developmental stages. Dorsal is up. The floorplate (arrowhead), motor neurons (circles) and dorsal root ganglia (asterisks) are indicated. *GPC4, GPC5* and *GPC5-like* were found in the floorplate. Only *GPC1* was found in mature commissural neurons (see Figure 1A). *GPC6* was not detected in the neural tube at the stages we examined. Adjacent sections to those shown in Figure 1A were hybridized with the sense probe for *GPC1* (F). Bar, 100 μm.

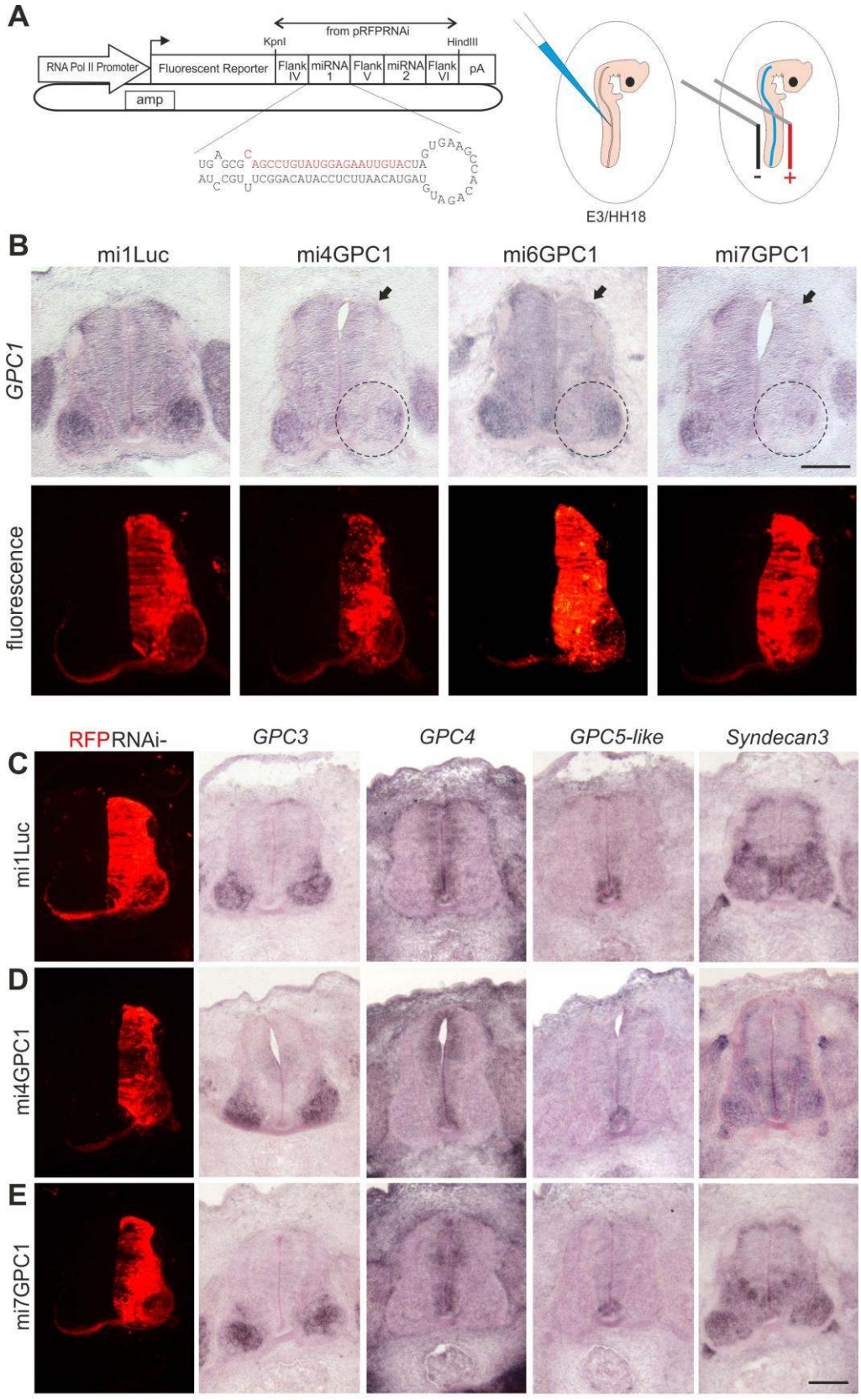
A
from pRFPRNAi
KpnI
HindIII
RNA Pol II Promoter
Fluorescent Reporter
Flank IV
miRNA 1
Flank V
miRNA 2
Flank VI
pA
amp
E3/HH18
B
mi1Luc
mi4GPC1
mi6GPC1
mi7GPC1
GPC1
fluorescence
RFPRNAi-
GPC3
GPC4
GPC5-like
Syndecan3
C
mi1Luc
D
mi4GPC1
E
mi7GPC1

Figure S2. Plasmid constructs encoding artificial miRNAs for specific GPC1 knockdown. Related to Figure 1 and 2.

(A) Schematic of the cell type-specific, traceable RNAi plasmid constructs used in this study (Wilson and Stoeckli, 2011). Red text indicates the sense strand of mi7GPC1. The 5' base of the sense strand is mismatched with the antisense sequence, so that it mimics the natural structure of miRNA30. Plasmids were injected and electroporated into the neural tube of chicken embryos at HH18. amp, ampicillin resistance; pA, SV40 polyadenylation signal.

(B) Three independent artificial miRNAs against *GPC1* (mi4GPC1, mi6GPC1, mi7GPC1) effectively knocked down GPC1 *in vivo*. Embryos were electroporated with pRFPRNAi vectors (Das et al, 2006). The electroporated half of the spinal cord (red fluorescence) displays reduced levels of *GPC1* expression compared to the non-targeted side; compare expression levels in the commissural neurons (arrows) and motor neurons (circles) between the two sides. A control miRNA against Luciferase (mi1Luc) had no effect on *GPC1* levels.

(C-E) To test specificity of knockdown, pRFPRNAi vectors were electroporated at HH17-18 and *in situ* hybridization (as indicated) was performed on spinal cord cross sections at HH26. Dorsal is up. The electroporated cells (right half of the spinal cord) were identified by red fluorescence. We observed no changes in the expression of *GPC3, GPC4, GPC5-like* or *Syndecan3* following electroporation of miRNAs against Luciferase (mi1Luc; C) or GPC1 (mi4GPC1, D; mi7GPC1, E). Bar, 100 µm.

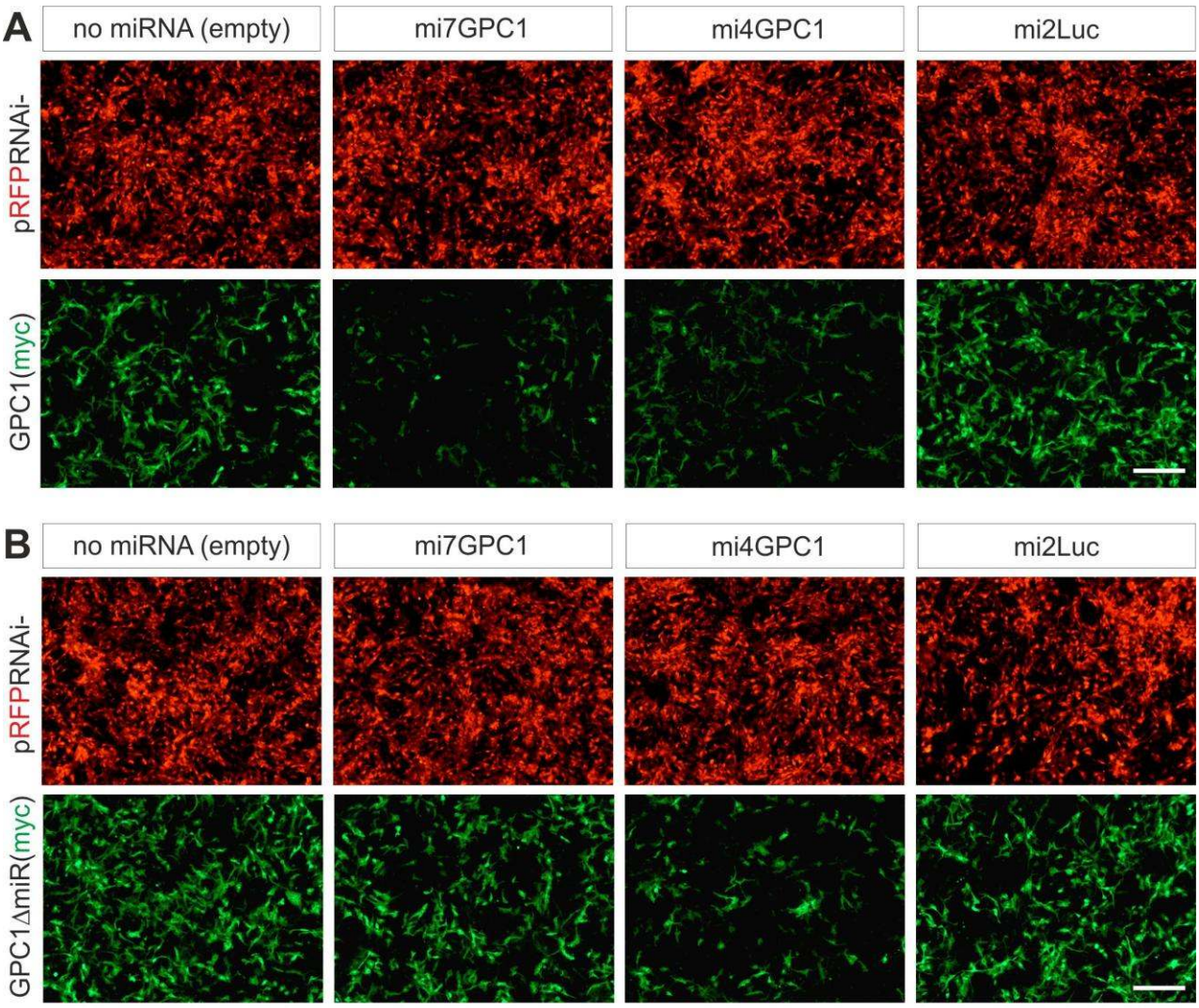

Figure S3. GPC1ΔmiR is resistant to knockdown by mi7GPC1. Related to Figures 1, 2, and 4. COS-7 cells were repeatedly transfected with pRFPRNAi vectors expressing the indicated miRNAs. The expression of RFP (red) showed that the majority of cells were transfected. Cells were then co-transfected with a construct driving the expression of (A) myc-tagged GPC1 or (B) myc-tagged GPC1ΔmiR. Immunolabeling for myc 24 hr later using the 9E10 antibody (green) revealed the ability of the different miRNAs to suppress expression of the different GPC1 constructs relative to control conditions. *GPC1* was effectively silenced by both mi4GPC1 and mi7GPC1, whereas *GPC1ΔmiR* was resistant to mi7GPC1 but still silenced by mi4GPC1 (which targeted a different sequence of GPC1). Bar, 200 μm.

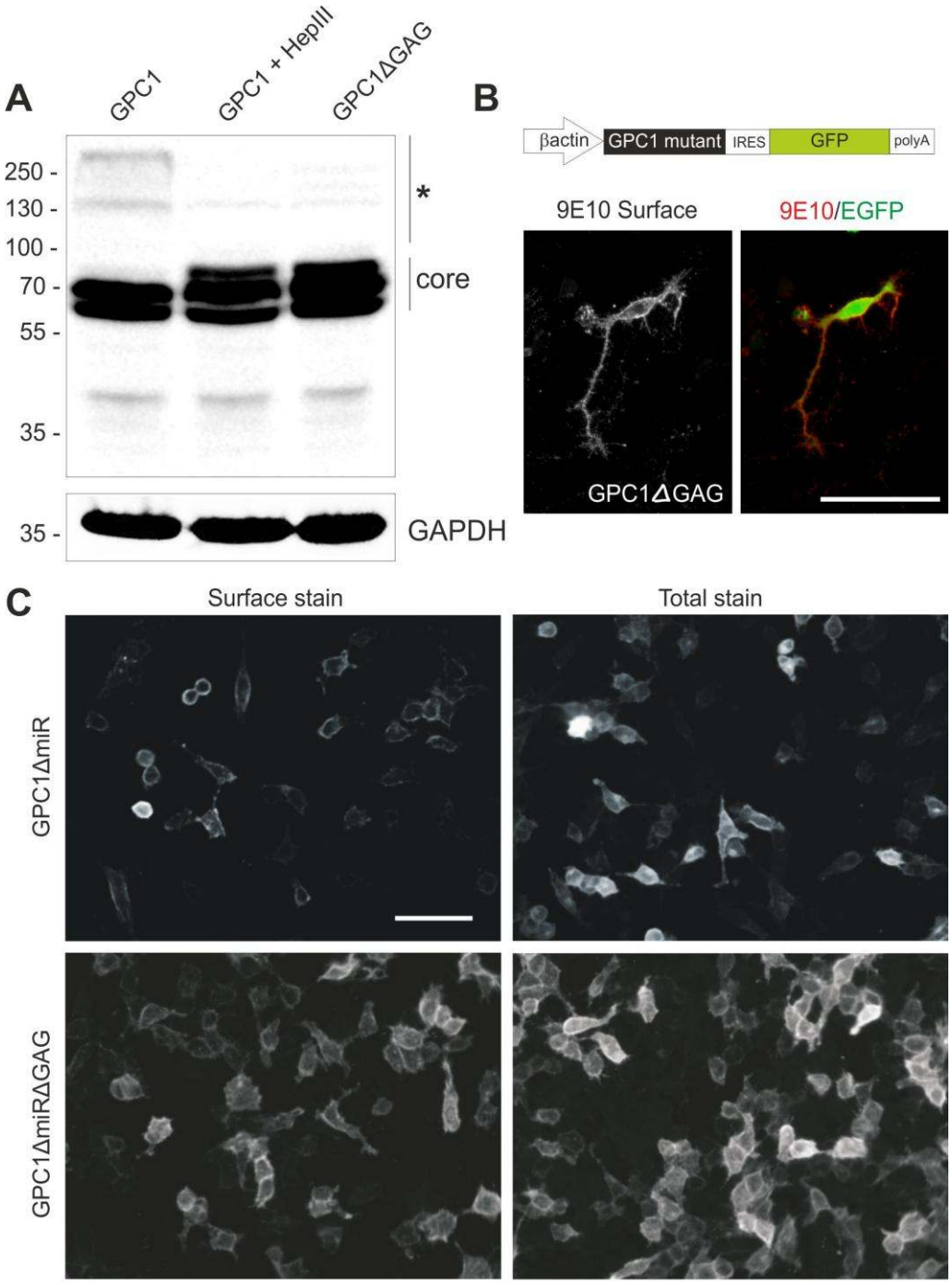

Figure S4. Mutant GPC1 constructs display the expected loss of glycanation and are correctly sorted to the cell surface. Related to Figures 1, 4, and 5.

(A) Western blot following heparinase III digestion of proteins in lysates obtained from transfected HEK293T cells. In control samples, cells were transfected with a myc-tagged *GPC1* construct and the

lysates were incubated with enzyme buffer alone. GPC1 was detected as three distinct groups of bands: high molecular weight bands migrating above 140 kDa (*), two bands between 60 and 70 kDa (core) and a weak immunoreactive band at ~42 kDa. Digestion with heparinase III resulted in the disappearance of the upper variants (*), characterizing them as glycanated versions of GPC1. Heparinase III treatment produced an immunoreactive band at ~80 kDa. The bands detected in lysates collected from cells transfected with myc-tagged *GPC1ΔGAG* were identical to those obtained following heparinase III digestion of wildtype GPC1, confirming that GPC1ΔGAG is not glycanated (but is otherwise processed identically). GAPDH in the cell lysates was assessed as a loading control.

(B-C) Cell surface staining of myc-tagged GPC1 mutant proteins on (B) dissociated commissural neurons obtained from electroporated embryos or (C) transfected HeLa cells. Surface proteins were detected by incubating the live preparations with 9E10 (anti-myc) for 2 hours at 4 ℃ prior to washing and fixation. Total staining revealed that GPC1 was also present intracellularly. Bar, 50 μm.

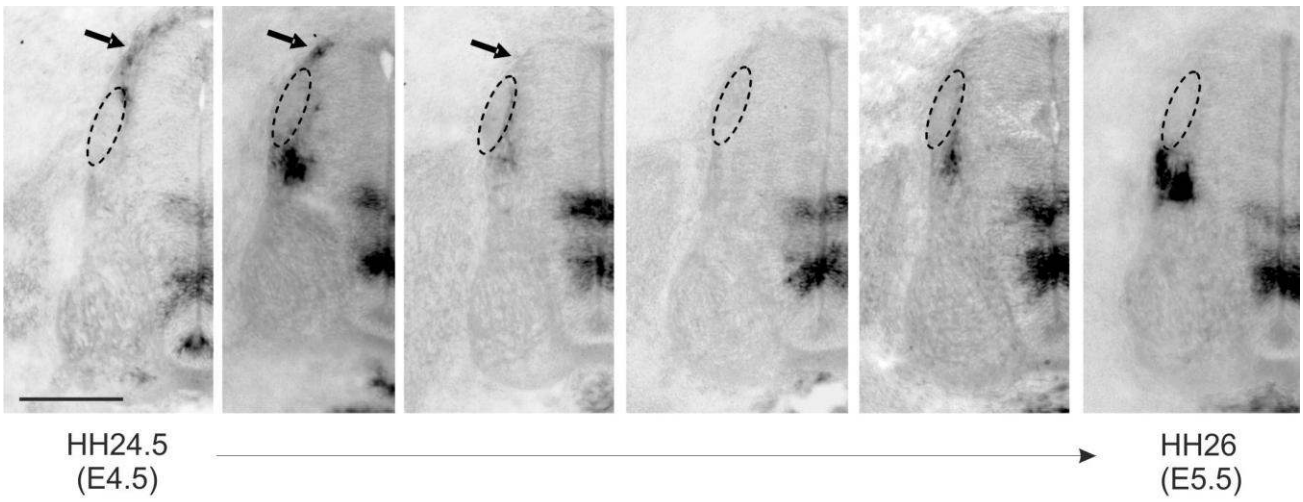

Figure S5. *Hhip* displays a dynamic expression pattern in the dorsal spinal cord. Related to Figures 4 and 5.

Images show *in situ* hybridization for *Hhip* in hemisections through the lumbar spinal cord between HH24.5 and HH26. Dorsal is up. At HH24.5, *Hhip* is located in the dorsolateral spinal cord in a position occupied by cell bodies of dI1 neurons (arrows). As development proceeds, *Hhip* expression shifts ventrally and at some point disappears from the dorsal spinal cord altogether (middle panel). By HH25.5, *Hhip* is strongly expressed in cells lying immediately ventral to the dorsal root entry zone (ovals). *Hhip* is stably expressed in two stripes in the ventromedial spinal cord throughout this period. Bar, 100 µm.

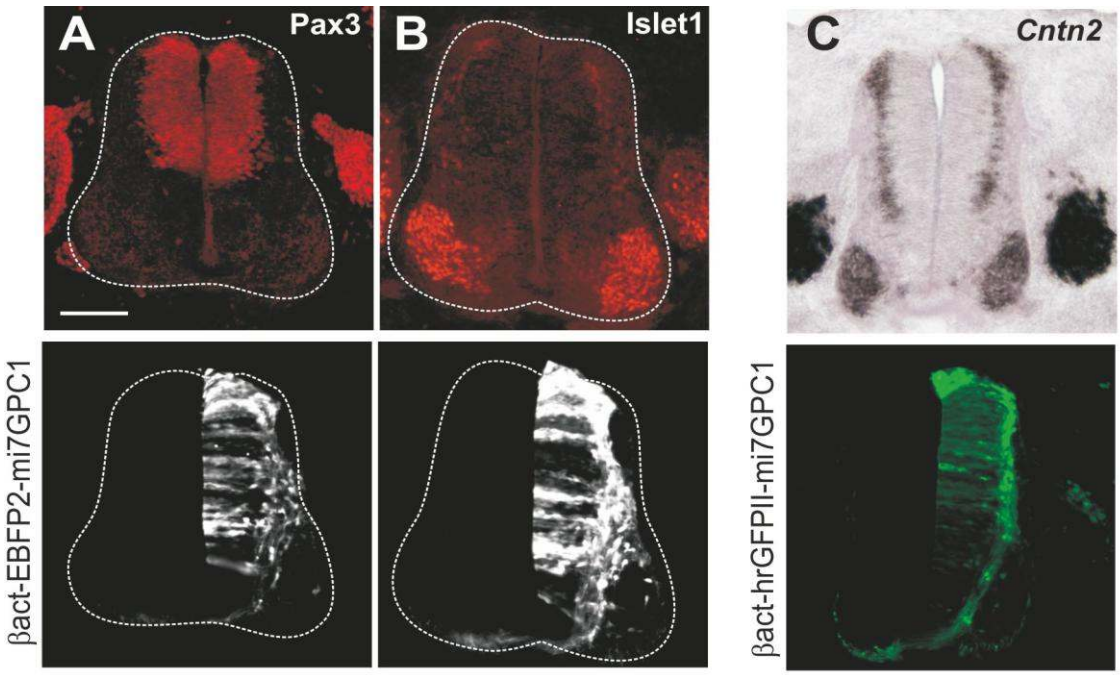

Figure S6. GPC1 is specifically required for the induction of *Hhip* expression in response to Shh signaling. Related to Figures 1, 4, 5, and 7.

Images show sections through the lumbar spinal cord taken from HH25-26 embryos electroporated with the indicated constructs at HH17-18. The electroporated cells (right half of the spinal cord) were identified by fluorescence. Dorsal is up. Silencing *GPC1* at HH17-18 did not grossly affect spinal cord patterning. Immunostaining for Pax3 (A) or Islet1 (B) showed no differences between control and electroporated sides of the spinal cord. Similarly, commissural neurons were found in their normal position after unilateral electroporation of mi7GPC1, when analyzed by *in situ* hybridization for *Cntn2* (C). Bar, 100 µm.

Table S1. Artificial miRNAs used in this study. Related to Figures 1 and 3.

Name	Target gene	Target sequence	Insertion site	Effective?
mi1Luc	firefly Luciferase	TGCTGCTGGTGCCAACCCTATT	First	Yes[1]
mi2Luc	firefly Luciferase	CGTGGATTACGTCGCCAGTCAA	First	Yes[2]
miShh	Sonic hedgehog	ACAAGAAACTCCGAGAGATTTA	Second	Yes[1,3]
miCntn2	Contactin2 / Axonin1	AAGGCACTTATGAGTGCGAGG	First	Yes[3]
mi1GPC1	Glypican1	ACGGCTTAGCTAATCAGATTAA	First	No
mi2GPC1	Glypican1	AGCGACTCTTCAAGCTGATGAA	First	No
mi3GPC1	Glypican1	GAAGTGAATTCGAAGCCATGAT	First	No
mi4GPC1	Glypican1	AAGGACTTGTACAGCGAGCTAC	First	Yes
mi5GPC1	Glypican1	AAGCCGTGCAGCAACTACTGCC	First	Weak
mi6GPC1	Glypican1	AAGCCGACCTGAACACCGAGTG	First	Yes
mi7GPC1	Glypican1	AAGCCTGTATGGAGAATTGTAC	First	Yes
mi8GPC1	Glypican1	AAGGCAACACGAGCCTTCATCG	First	No

[1] Das et al., 2006

[2] Khvorova et al., 2003

[3] Wilson and Stoeckli, 2011

Table S2. Phenotypes in combinatorial knockdown experiments. Related to Figure 3.

Condition[a]	N (embryos) n (DiI sites)	Normal (%)	Ipsilateral errors (%)	Stalling in FP (%)	Contralateral stalling/turning errors (%)
Hox-EBFP2-mi1Luc + *Math1-EGFPF-mi1Luc*	N=12 n=116	66.4	0.0	7.8	26.7
Hox-EBFP2-miShh + *Math1-EGFPF-mi1Luc*	N=14 n=116	73.3	0.0	5.2	25.0
Hox-EBFP2-mi1Luc + *Math1-EGFPF-mi7GPC1*	N=20 n=156	61.5	0.6	14.7	24.4
Hox-EBFP2-miShh + *Math1-EGFPF-mi7GPC1*	N=19 n=99	50.5*	0.0	15.1	41.4*
Hox-EBFP2-mi1Luc + *Math1-EGFPF-miCntn2*	N=12 n=84	65.5	2.4	4.8	28.6
Hox-EBFP2-miShh + *Math1-EGFPF-miCntn2*	N=9 n=66	71.2	0.0	10.6	28.8

[a]Injection mix: *Hox-EBFP2-miR* (0.5 µg/µl) + *Hox-EBFP2* (0.5 µg/µl) + *Math1-EGFPF-miR* (0.35 µg/µl) + *Math1-EGFPF* (0.35 µg/µl) in PBS with 0.04% trypan blue; bilateral electroporation. A mixture of plasmids expressing fluorescent protein alone or fluorescent protein and miRNA was used to ensure the same total amount of DNA was electroporated in all cases.

* $p<0.05$, Fisher exact test. Statistical tests were performed by comparing raw phenotype numbers for subthreshold injections of each miRNA alone with those obtained after simultaneous partial knockdown.

Table S3. Phenotypes following electroporation at HH12-14. Related to Figure 3.

Condition	N (embryos) n (DiI sites)	Normal (%)	Ipsilateral errors (%)	Stalling in FP (%)	Contralateral stalling/turning errors (%)
βact-hrGFPII-mi2Luc	N=9 n=80	68.8	2.5	10.0	22.5
βact-hrGFPII-mi7GPC1	N=7 n=81	49.9*	4.9	22.2*	37.0*

* $p<0.05$; Fisher exact test.

Supplemental Experimental Procedures

Animals

Fertilized chicken eggs were obtained from a local supplier and embryos were staged according to Hamburger and Hamilton (1951). All electroporations were performed at HH17-18, except in the experiments shown in Table S3.

Quantification of axon guidance phenotypes

At least 10 embryos were examined per condition. Fast DiI (Molecular Probes) was dissolved in ethanol at 5 mg/ml and focally injected. Only DiI injections sites that were in the appropriate location in the dorsal-most part of the spinal cord, and within the region expressing fluorescent protein, were included in the analysis. In the *Math1-EGFPF-miR* experiments, it was impossible to directly assess individual trajectories of the fluorescent axons due to the large number of axons labeled using this technique. Thus, we continued to use DiI injections to label smaller cohorts of commissural axons. At individual injection sites, the percentage of axons displaying abnormalities was estimated by a person blind to the experimental condition, and the injection site was classified as showing a 'normal' phenotype if the axons crossed the floorplate and turned rostrally along the contralateral floorplate border. In a single abnormal DiI injection site, it was possible that more than one error class was observed (for example, both 'ipsilateral' errors and 'floorplate stalling' errors).

Cloning

All primer sequences are available on request.

Artificial miRNAs

pRFPRNAiC (Das et al., 2006) was obtained from ARK-Genomics. The other plasmids, each containing an RNA polymerase II promoter/enhancer, fluorescent protein and miRNA expression cassette were synthesized as described (Wilson and Stoeckli, 2011). Artificial miRNAs against our genes of interest were generated by PCR as described (Das et al., 2006; Wilson and Stoeckli, 2011) and cloned into the first or second miRNA insertion sites, using NheI/MluI or MluI/SphI, respectively (Table S1). Eight candidate miRNAs against GPC1 (mi1GPC1-mi8GPC1) were tested *in vivo* by electroporating *pRFPRNAi* vectors and assessing *GPC1* expression by *in situ* hybridization (Figure S2). GPC1 was knocked down by mi4GPC1, mi6GPC1 and mi7GPC1. As negative controls, we used miRNAs against firefly Luciferase (mi1Luc-mi2Luc; Table S1).

Glypican1 constructs

Total RNA was extracted from HH25-26 chicken embryos using Trizol reagent (Invitrogen) prior to reverse transcription and PCR. The *GPC1* PCR product was cloned into pGEM-TEasy (Promega) and sequenced (Genbank accession number KF040585). The signal sequence was predicted using SignalP 3.0. Myc or HA tags were inserted by first creating a XhoI site by silent mutagenesis, then inserting a PCR product generated using the GPC1 reverse primer together with a forward primer that incorporated an in-frame myc or HA sequence and an engineered flanking XhoI restriction site.

*GPC1*Δ*miR* was mutagenized according to current considerations for miRNA target selection and cleavage (Brodersen and Voinnet, 2009). An *in vitro* protocol used to verify that the construct was resistant to knockdown by mi7GPC1 is given in detail elsewhere (Wilson and Stoeckli, 2011; Figure S3).

In the GPC1ΔmiRΔGAG mutant, three serine residues (S483, S485, S487) were converted to tyrosines. We performed Western blots to confirm the loss of glycanation in this mutant (Figure S4A and see below).

In GPC1ΔmiRΔGAGΔShh, 10 residues (T182, D183, E184, D187, K191, H192, Q195, K197, E201, D205) were additionally mutated to alanines. These residues were equivalent to those whose mutation completely blocked the ability of Dally-like protein (Dlp; *Drosophila* glypican) to mediate Hedgehog signaling (Kim et al., 2011). Western blot analysis indicated that this construct lacked some post-translational modifications of the core protein, compared to GPC1 and GPC1ΔmiRΔGAG. Unlike GPC1 and GPC1ΔmiRΔGAG, GPC1ΔmiRΔGAGΔShh did not co-IP with Shh, supporting the idea that GPC1ΔmiRΔGAGΔShh cannot mediate Shh signaling (Figure 5C).

For expression analyses, the *GPC1* constructs were cloned into *pcDNA3.0*, *pcDNA3.1* (Invitrogen) or *pMES* (C. Krull). The *pMES* plasmid contains an internal ribosomal entry site (IRES) followed by EGFP, thus allowing visualization of the transfected cells. We ensured that the modified GPC1 constructs were properly expressed at the cell surface using an *in vitro* approach (Figure S4B-C). COS-7 (not shown) and HeLa cells were transfected using Lipofectamine 2000 (Invitrogen) with *pcDNA3* plasmids containing the constructs, and allowed to grow for 2 days. Alternatively, the *pMES* constructs were electroporated into the chicken neural tube and dissociated commissural neuron cultures were prepared as described below. We then labeled myc-tagged GPC1 at the cell surface by incubating the live preparations with 9E10 (anti-myc) at 4˚C for 2 hours. Unbound antibody was washed away before cells were fixed in 4% paraformaldehyde (PFA) for 30 mins, blocked in 10% fetal calf serum (FCS) in PBS for 30 mins before applying an appropriate fluorescent secondary antibody. Total stains were performed by simultaneously blocking and permeabilizing fixed cells in 10% FCS/PBS containing 0.1% Triton-X100, prior to applying the 9E10 antibody.

Shh-FLAG, Hhip, Ptc∆loop2, Smo-M2, Gli1 and Gli2 constructs

A chicken *Shh* construct containing an internal FLAG-tag downstream of the signal sequence was generated by PCR using a similar strategy to that described above for the tagged *GPC1* constructs. Myc-tagged mouse *Hhip* was amplified from *Hhip(myc)-pcDNA3.0* (A. McMahon) then subcloned into *pMES*. Expression constructs containing *Ptc∆loop2* (a hedgehog-insensitive, dominant repressor of Smo; Briscoe et al., 2001), *Smo-M2* (a constitutively active form of Smo; Hynes et al., 2000), mouse *Gli1* and mouse *Gli2* were kindly provided by J. Briscoe.

In situ hybridization and immunolabeling

In situ hybridization was performed as described (Mauti et al., 2006). We used probes produced from chicken cDNAs that were previously cloned in the lab, or ESTs obtained from Geneservices Ltd. The sequences used were fragments of *Glypican1* (1.4 kb), *Contactin2 (Axonin1*) (1.5 kb), *Hhip* (1.3 kb), *Patched1* (0.8 kb), *Sfrp1* (0.8 kb) and EST fragments of *Glypican3* (ChEST 410e19), *Glypican4* (ChEST 335n21), *Glypican5* (ChEST 59j20), *Glypican5-like* (ChEST 67l17), *Glypican6* (ChEST 374m20), *Syndecan3* (ChEST 993n9), *Frizzled3* (ChEST 557b17) and *Boc* (ChEST 38e3).

Immunolabeling of 25-µm-thick cryostat sections was performed as described (Perrin et al., 2001; Wilson and Stoeckli, 2011). Dissociated commissural neurons were obtained from the dorsal 1/5 of the spinal cord from HH25-26 embryos and grown for 2 days on 8-well LabTek slides (Nunc) coated with poly-Lysine (10 µg/ml; Sigma). The growth medium was as previously described (Niederkofler et al., 2010), supplemented with 5% fetal calf serum. After fixation in 4% PFA for 30 minutes at room temperature, cultures were stained with goat anti-GPC1 (sc-33923; Santa Cruz Biotechnology) and rabbit anti-Axonin1 (anti-Cntn2). Other primary antibodies used in this study were: mouse anti-myc (9E10), mouse anti-Pax3, mouse anti-Islet1 (40.2D6), and goat anti-GFP-FITC (Rockland). All

monoclonal antibodies were obtained from Developmental Studies Hybridoma Bank (University of Iowa, USA). Fluorophore-conjugated secondary antibodies were purchased from Jackson ImmunoResearch Laboratories or Invitrogen.

Analysis of *Hhip* expression patterns

Hhip normally displays a very dynamic expression pattern in the dorsal spinal cord in the 24 hours between HH24-27 (Figure S5; Bourikas et al., 2005). This highly dynamic expression pattern made it impossible to accurately compare *Hhip* expression levels between different embryos, even after careful staging of embryos based on gross morphological criteria. Rather, we used the non-electroporated side of the spinal cord as an internal control for the appropriate location and intensity of *Hhip* expression. Sections in which there was no dorsal *Hhip* expression on the non-electroporated side (for example, Figure S5, middle) were excluded from this analysis. Sections were obtained from 4-7 embryos in each condition.

Digital analysis of *Hhip* staining intensities was performed using ImageJ software. Images were converted to 8-bit, a threshold was applied, and the integrated density of pixels above the threshold in the dorsal or medial spinal cord, on the control (cont) and electroporated (elect) sides, was measured. These measurements provided the pixel intensity (PI) values. A ratio of PI^{elect}:PI^{cont} was calculated for the dorsal and medial areas in each image. A ratio of 1 indicated symmetrical staining, and a ratio of <1 indicated reduced staining on the electroporated side. The average dorsal and medial ratios for each condition were calculated and presented as mean +/- SEM. To assess the 'symmetry' of dorsal *Hhip* staining in each treatment, the dorsal ratios were first subjected to a single sample t-test against a hypothetical mean of 1 (shown in green in Figure 4G and Figure 5E). To assess the ability of the different rescue treatments to restore symmetry, the dorsal ratios were compared between the relevant groups using two-sample t-tests.

Western blots and Co-immunoprecipitations

Testing glycanation of GPC1∆miR∆GAG

HEK293T cells in 10-cm dishes were transfected with *pcDNA3.0* vectors containing myc-tagged *GPC1* or *GPC1∆miRΔGAG* (14 µg DNA per dish), using the calcium phosphate method. Two days later, the cells were scraped off the dish, centrifuged, washed in PBS and lysed in 500 µl of lysis buffer (150 mM NaCl, 0.1% Triton X-100, protease inhibitors (Roche), 20 mM Tris, pH 8.0) on ice for 30 minutes. An aliquot of the GPC1 lysate (30 µl) was supplemented with 4 mM $CaCl_2$, then treated with 1U heparinase III (Sigma; reconstituted in 0.1 mg/ml BSA, 4 mM $CaCl_2$, 20 mM Tris-HCl, pH 7.5) for 4 hours at 37 ℃. For the control sample, GPC1 lysate was incubated with enzyme buffer alone. Samples were analyzed by SDS-PAGE and Western blot using the 9E10 antibody against myc (Figure S4A).

Co-immunoprecipitations

Due to a lack of antibodies for detecting endogenous Shh in Western blots from chicken spinal cord lysates, we instead assessed GPC1-Shh interactions using tagged constructs. HEK293T cells were transfected as described above. We used pShh-FLAG alone, pGPC1-HA alone, or co-transfected both. A mock transfection condition (no DNA) was included as an additional negative control. Cells were harvested 48 hr later and lysed in 900 µl of lysis buffer on ice for 30 mins. The lysates were incubated with monoclonal anti-FLAG M2 affinity gel (Sigma) at 4 ℃ overnight. Beads were washed 4 times with lysis buffer and eluted in 2X Non-Reducing Sample Buffer (ThermoScientific) after heating at 95 ℃ for 3 mins. SDS-PAGE and Western blotting was conducted according to standard techniques using a 12% gel and PVDF membrane.

We used a similar method to assess interactions between the myc-tagged mutant GPC1 constructs and Shh (Figure 5C). Immunoprecipitation was performed using anti-FLAG M2 affinity gel.

For detection of proteins, we used goat antibodies (Santa Cruz Biotechnology, Inc) against Shh (sc-1194: 1:1000) and GPC1 (sc-33923; 1:500), as well as goat anti-FLAG (ab1257; 1:10,000), rabbit anti-GAPDH (ab9485; 1:2500) (Abcam) and mouse anti-myc (9E10; 1:1000) (DSHB).

Supplemental References

Brodersen, P., and Voinnet, O. (2009). Revisiting the principles of microRNA target recognition and mode of action. Nat Rev Mol Cell Biol *10*, 141–148.

Khvorova, A., Reynolds, A. and Jayasena, S.D. (2003) Functional siRNAs and miRNAs exhibit strand bias. Cell *115***,** 209–216.

Perrin, F.E., Rathjen, F.G., and Stoeckli, E.T. (2001). Distinct subpopulations of sensory afferents require F11 or axonin-1 for growth to their target layers within the spinal cord of the chick. Neuron *30*, 707–723.